NOVA SCHOOL OF SCIENCE & TECHNOLOGY

DEPARTAMENT OF CHEMISTRY

MARCOS DE SÃO JOSÉ ROSA RAMALHO FRAZÃO CORREIA

BSc in Biochemistry

PRODUCTION OF NEW ANTIMICROBIAL NANOMATERIALS WITH SYNERGISTIC PROPERTIES FOR DRUG DELIVERY AGAINST INFECTIOUS DISEASES

MASTER IN BIOMATERIALS AND NANOMEDICINE

NOVA University Lisbon

September, 2024

DEPARTAMENT OF
CHEMISTRY

PRODUCTION OF NEW ANTIMICROBIAL NANO-MATERIALS WITH SYNERGISTIC PROPERTIES FOR DRUG DELIVERY AGAINST INFECTION DISEASES

MARCOS DE SÃO JOSÉ ROSA RAMALHO FRAZÃO CORREIA

BSc in Biochemistry

Adviser: Dr. Elisabete Oliveira Marques
Assistant Researcher (CEEC), Chemistry Department, NOVA School of Science and Technology, NOVA University Lisbon, Portugal.

Co-advisers: Prof. Dr. Carlos Lodeiro
Full Professor, Chemistry Department, NOVA School of Science and Technology, NOVA University Lisbon, Portugal.

MASTER IN BIOMATERIALS AND NANOMEDICINE

NOVA University Lisbon
September, 2024

PRODUCTION OF NEW ANTIMICROBIAL NANOMATERIALS WITH SYNERGISTIC PROPERTIES FOR DRUG DELIVERY AGAINST INFECTION DISEASES

Aos meus avôs, que sempre foram exemplo de como a simplicidade torna a vida bela.

.

ACKNOWLEDGMENTS

The presented work involved a lot of hours in the lab, in the office, and at home. However, more than the work done individually, this would most certainly not be achieved alone. Therefore, hereby I acknowledge those whose role in my life was undeniably crucial throughout this journey.

First and foremost, I would like to express my deeply gratitude to my supervisors, Dr. Elisabete Oliveira and Prof. Carlos Lodeiro, to whom I am incredibly grateful for their constant support and guidance, all the life advices, but mostly, for becoming role models that I most certainly look up to. I am especially grateful to Dr. Elisabete Oliveira for making me feel comfortable since day one and for always keeping herself close to me and my work. Her hard work was a great motivation for me throughout this year, and her sincerity and patience made me grow both professional and personally. I would also like to thank Prof. Carlos Lodeiro for inviting me to be part of the BIOSCOPE Research Group, which allowed me to expand my areas of knowledge in all the scientific congresses, but also for showing me the importance in being critical in life and not being afraid to take risks.

Also, this work was supported by the Associate Laboratory for Green Chemistry - LAQV which is financed by national funds from FCT/MCTES (LA/P/0008/2020 DOI 10.54499/LA/P/0008/2020, UIDP/50006/2020 DOI 10.54499/UIDP/50006/2020 and UIDB/50006/2020 DOI 10.54499/UIDB/50006/2020) as well as the Scientific Society PRO-TEOMASS (Portugal) for funding support (General Funding Grant 2023-2024).

I would also like to extend my gratitude to all the members of the BIOSCOPE Research Group. To Prof. José Luís Capelo and Dr. Hugo Santos, whose refreshing presence always brightened my day whenever I had the good fortune of crossing paths with them. To Dr. Javier Lodeiro, thank you for warmly welcoming me into the lab and for sharing not only valuable scientific knowledge but also conversations that uplifted my spirits. To André Figueiredo, which

had the immense patience to guide me through my long hours of figure creation and who planted in me the passion for squash. To Inês Domingos, Dr. Luís Carvalho, Dr. Sílvia Nuti, Frederico Duarte, and Gonçalo Pedro, who shared this year with me and welcomed me in their routine filled with hard work, great talks, and great scientific congresses. Finally, I would like to give a special thanks to Joana Galhano, who closely guided me throughout this year and taught me so much in and outside the lab, that I will certainly make the most of it in the future.

Furthermore, as I am nothing without my friends, I cannot go further without thanking them. To my recent friends that helped go through these last two years, Tito, Rafa, Pris, Vânia, and Alex. For so warmly welcoming into this mind-blowing faculty, for all the lunches, afternoons at the campus (where else…), late night calls, for showing me what Lisbon truly is, but most of all, thank you for the moments where nothing made sense, yet it all made sense together. To my northern friends, Joana, Cláudia, Quim, Pablo, Edu, Tommy, Mafalda, Meireles. For these hard, but epic five years, for having made me call Porto my new hometown, but especially, for having, each one in your very own way, made me into what I am today. And finally, to my long-lasting friends, the S.P.A. Although I might just see you once a year, you will always be in my heart, along with all the adventures that have shaped us and those still to come.

To my dear Érica, who has the extraordinary capacity of supporting me no matter what, who is constantly trying to turn me into a better man, and who always showed so vividly her pride on my small achievements. Here's to all the distant times we lived through and all the close ones that await us in the future.

Finally, I could not end without thanking my family, who supported me over my entire life and to whom I so desperately want to get some independence. For all the "paitrocínios", for all the stress in guaranteeing my well-being, for the countless moments of stupidity and nonsense, and for believing in my capacities more than even myself.

“Do not claim you have no time, admit that you have other priorities.” (Unknown).

ABSTRACT

Antimicrobial resistance (AMR) is one of the most concerning issues of today, posing a global public health threat already warned by the WHO. As one of the principal agents of mucosal and systemic infections, *Candida albicans* is a fungus that, when disseminated, can lead to life-threatening infections and has increased its incidence in the last decades, showing resistance to some current treatments. Considering this and recognizing the difficulty on creating new drugs, nanomaterials have been addressed as an answer to AMR.

This work has addressed the potential of silver-copper core mesoporous silica shell nanoparticles (AgCuMNs) against *C. albicans*, starting by synthesizing the nanoparticles (NPs), loading Amphotericin B (AMB), a drug used in *C. albicans* infections, and then, testing the resulting nanomaterials against the fungus. Indeed, we were able to synthesize 49 nm diameter AgCuMNs with 2.52 nm diameter pores and a high surface area due to the mesoporous silica shell. Then, by achieving a loading percentage of 90.1%, we were able to prove that mesoporous silica can indeed retain drugs, increasing massively their solubility, thus creating easier ways to administrate them.

Finally, our nanosystems were tested against *C. albicans*. Interestingly, not only did the drug loaded into the nanosystems showed effects, but also the AgCu core demonstrated synergetic effects with the drug, making the loaded AgCuMNs as the most effective nanosystem. Indeed, this nanosystem was able to have a Minimum Inhibitory Concentration (MIC) of 6.25 µg/mL, which corresponds to a concentration of the drug of 0.089 µg/mL. Overall, AgCuMNs showed a great potential to be used as drug-delivery systems, hopefully helping the fight against antimicrobial resistance.

Keywords: Antimicrobial Resistance, *Candida albicans*, AgCu alloy, mesoporous silica, drug-delivery system.

RESUMO

Resistência antimicrobiana é uma das questões mais preocupantes da atualidade, representando uma ameaça global à saúde pública já alertada pela OMS. Como um dos principais agentes de infeções mucosas e sistémicas, *C. albicans* é um fungo que, quando disseminado, pode causar infeções potencialmente fatais, tendo aumentado a sua incidência nas últimas décadas e demonstrando resistência a alguns tratamentos atuais. Considerando este cenário e reconhecendo a dificuldade em desenvolver novos fármacos, os nanomateriais têm sido abordados como uma resposta à resistência antimicrobiana.

Este trabalho focou-se no potencial de nanopartículas com núcleo de prata-cobre revestido com sílica mesoporosa (AgCuMNs) contra *C. albicans*, começando pela síntese das nanopartículas (NPs), o carregamento de Amphotericin B (AMB), um fármaco utilizado em infeções de *C. albicans* e, posteriormente, o teste dos respetivos nanomateriais contra o fungo. De facto, sintetizámos AgCuMNs com 49 nm de diâmetro, poros de 2.52 nm de diâmetro e uma elevada área de superfície devido à sílica mesoporosa. Atingimos uma percentagem de loading de 90.1%, comprovando que a sílica mesoporosa consegue, de facto, reter fármacos, aumentando consideravelmente a sua solubilidade e, facilitando, assim, a sua administração.

Por fim, os nanosistemas foram testados contra *C. albicans*. Curiosamente, não só a AMB carregada nos nanosistemas demonstrou efeitos, como também o núcleo de AgCu apresentou efeitos sinérgicos com o fármaco, tornando as AgCuMNs carregadas no nanosistema mais eficaz. De facto, este nanosistema apresentou um MIC de 6.25 µg/mL, o que corresponde a uma concentração de fármaco de 0.089 µg/mL. Em geral, as AgCuMNs mostraram um grande potencial como sistemas de transporte de fármacos, contribuindo, assim, para a luta contra a resistência antimicrobiana.

Palavras chave: Resistência antimicrobiana, *C. albicans*, AgCu alloy, sílica mesoporosa, sistemas de transporte de fármacos.

CONTENTS

LIST OF FIGURES

List of Tables

ACRONYMS

BCS	Biopharmaceutics Classification System.
BET	Brunauer-Emmett-Teller.
BJH	Barrett-Joyner-Halenda
CDC	Centers for Disease Control and prevention.
CFU	Colony Forming Unit
DLS	Dynamic Light Scattering.
EDS	Energy Dispersive Spectrometry.
FTIR	Fourier Transform Infrared.
FDA	Food and Drug Administration.
HPV	Human Papillomavirus.
HSV	Herpes Simplex Virus.
MCM	Mobile Composition of Matter.
MFC	Minimum Fungicidal Concentration.
MHB	Mueller-Hinton Broth.
MIC	Minimum Inhibitory Concentration.
MNP	Mesoporous silica Nanoparticle.
OD	Optical Density.
PEG	Polyethylene Glycol.

QD	Quantum Dot.
ROS	Reactive Oxygen Species.
RTI	Reproductive Tract Infection.
SBA	Santa Barbara Amorphous.
SDA	Sabouraud Dextrose Agar.
SEM	Scanning Electron Microscopy.
SPION	Superparamagnetic Iron Oxide Nanoparticles.
STI	Sexually Transmitted Infection.
STM	Scanning Tunneling Microscopy.
TEM	Transmission Electron Microscopy.
VVC	Vulvovaginal Candidiasis.
WHO	World Health Organization.

1

INTRODUCTION

1.1 Nanotechnology

In a relatively short period of time, nanotechnology has taken control of multiple industries worldwide, defining the era we live in. From the commonly used mobile phone to medicine, nanotechnology has gained significant importance in our daily life, englobing areas such as physics, biology, and chemistry[1,2].

Although the Romans and some cultures throughout history had used nanoparticles in diverse applications, notably in staining objects, the awareness that such small particles existed or were even possible to manipulate was only first described in 1959 by Richard Feynman in his famous lecture "There's Plenty of Room at the Bottom". The now common term "nanotechnology" was first introduced by Norio Taniguchi in 1974 and the first book about nanotechnology was published in 1986 by K. Eric Drexler with the name of "Engines of Creation: The Coming Era of Nanotechnology". Indeed, it was in the 1980s, with the creation of the first Scanning Tunneling Microscope (STM), enabling the visualization and manipulation of single atoms that the field began to grow, culminating in 1990 with Don Eigler being able to manipulate single Xenon atoms to form the IBM logo. Carbon Dots were subsequently discovered by Xu et al. in 2004, marking another milestone. Commercial applications of nanotechnology also began to emerge in the early 2000s, raising public awareness of the field allied with some controversy. Then, during the 2010s the nanomaterial applications continued, highlighting its efficiency and sustainability in solar and fuel cells, with notable achievements culminating in the 2023 Nobel Prize in Chemistry being awarded for the discovery and development of quantum dots[1,3–6].

The prefix "nano" comes from the Greek *nános*, meaning "dwarf" and stands for something very small, also referring, in the metric system, to the thousand-millionths of a determined unit (10^{-9})[7]. Taniguchi defined nanotechnology as the "processing of separation, consolidation, and deformation of materials by one atom or one molecule"[1]. Nevertheless, the definition has evolved through time and, nowadays, it is defined as the intentional design, production, characterization and application of materials, structures, and systems by controlling their shape and size in the nanoscale range (from 1-100 nm)[8]. Although this definition is widely accepted, in some fields like medicine, it can be more flexible, including nanodrug formulations up to 200 nm or more[6].

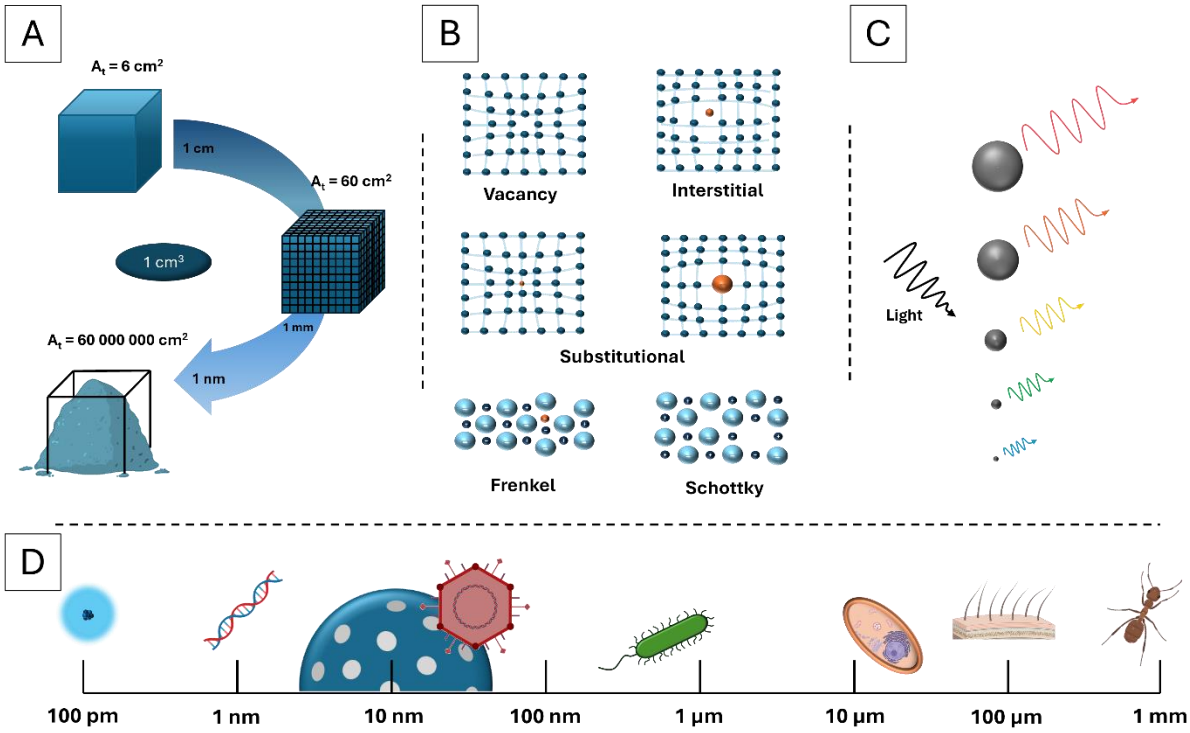

Figure 1 - The nano world. Main characteristics affected for nanomaterials: (A) higher surface-volume ratio; (B) fewer crystalline defects; and (C) quantum effects. (D) Scale comparing nanoparticles with other biological structures.

Due to their small sizes, nanoparticles exhibit distinct physicochemical properties from their bulk material's fundamental properties. Essentially, when entering the nanoscale sizes, there are properties that will be massively affected, especially due to the significantly higher surface-volume ratio, the fewer crystalline defects, and the appearance of quantum effects. These characteristics are depicted in Figure 1 (A-C) and will have an impact mainly on the materials' structural, optical, mechanical, thermal, and electromagnetic properties. Some consequences are that the increased contact surface will lead to stronger interactions and, as

electrical and optical properties undergo changes, fields like electronics and bioimaging will make use of their unique properties[4].

Nanomaterials can be divided into four main categories: carbon-based; inorganic-based; organic-based; and composite-based[4]. Carbon-based nanomaterials, made exclusively of carbon, exhibit exceptional electronic and mechanical properties in various forms such as tubes, sheets, or spheres.[9–11] Inorganic-based nanomaterials are composed essentially of metals and non-metals such as Ag, Au, Si, Se, Te, and others, englobing the famous Quantum Dots. Moreover, organic-based nanomaterials are composed of organic molecules like lipids, known for their bioavailability and non-toxicity, making them extensively studied in drug delivery systems. Finally, composite-based nanomaterials are mainly made of a polymer, ceramic or metal matrix, being then reinforced with other desirable molecules or compounds, having modifiable surface properties in a relatively easy way.[11]

1.2 Metal core-shell mesoporous silica nanoparticles (Metal@MNs)

Core-shell nanoparticles are hybrid nanomaterials that, by combining different materials, can integrate diverse functionalities into a single nanoparticle. This term was first described in the early 1990s, having become very popular in the last years as it has numerous applications in a wide range of areas. This has special importance regarding metal nanoparticles as they are poorly suited for many practical applications, but their coating allows them to be integrated into functional devices[12–14].

Typically, it consists of an original nanoparticle (core) surrounded by one coating layer (shell), but there can be made several combinations, allowing practically unlimited possibilities. Generally, there are three main types of core-shell nanoparticles: core-shell, hollow core-shell and yolk-shell, also known as rattle core-shell. Briefly, the first one is when the core is directly connected to the shell, hollow core-shell, as suggested by the name, is when the core is removed, creating a hollow space inside the nanoparticle and yolk-shell nanoparticles can be described as a mid-term of the previous two, having a core@void@shell structure. Moreover, adding to the fact that it is possible to have multiple cores, multiple shells, and many possible shapes, there are different types of cores, such as dense and porous and different types of shells, such as continuous and discontinuous dense shells and porous shells [12,13,15].

When designing a core-shell system, it is crucial to think thoroughly about several factors. Firstly, the selection of the materials for both the core and shell is critical. Secondly, it must be determined which type of core and shell is desired and parameters such as core size, thickness of the shell and so on. Finally, there are details that must be understood and chosen such as morphology and size, pore size and surface modification. This will be of major importance as, in some cases, the formation of the shell can make the core exhibit new chemical or catalytic reactivity, which might be something desired or not [12,13,15].

Regarding Metal core-shell nanoparticles, the shell will have several functions. Essentially, the shell is a physical separation between the core and the outer medium, so, it will protect the core from environmental fluctuations and external factors such as oxidation and temperature, which will in turn make them more stable. Furthermore, it will provide specific properties according to the desired application, such as biocompatibility, tunable refractive index and surface plasmon band, and increase or decrease of reactivity. Finally, the shell itself may have increased affinity to or be functionalized with specific molecules, allowing to identify target molecules, creating superstructures, and working as improved imaging markers [12,13,16–18].

Generally, a shell can be made of metals, metal oxides, inorganic and organic compounds, and polymers. Amongst the most used are Au, TiO_2, silica, carbon, and polyethylene glycol (PEG)[17,19,20]. These shells enable metal nanoparticles to gain desired properties and be effectively used in areas such as catalysis, electronics, environmental remediation and biomedicine as several theranostics ways[13,15,17,21–23].

From these materials, silica-based nanomaterials have become one of the largest nanomaterials produced worldwide as they present impressive physicochemical properties and are considered safe by the US Food and Drug Administration (US-FDA). These aspects enable their application in a wide range of areas, such as agriculture, environmental remediation, cosmetics, industry and biomedicine[24–26].

Silicon dioxide (SiO_2), commonly known as silica, is one of the most abundant materials on earth, being able to be obtained from either several minerals or synthetic production. Usually, the Si atom presents a tetrahedral coordination, with four oxygen atoms around the central Si atom, which in turn allows the possibility of other arrangements such as siloxane (Si-O-Si) and silanol (Si-OH) functional groups[27,28].

Therefore, silica nanoparticles, more specifically, mesoporous silica nanoparticles (MNs) are highly required given their colloidal, chemical and thermal stability, biocompatibility, controlled particle and pore sizes, and large surface area[27,29,30]. By some, silica is considered ideal

for encapsulating metal nanoparticles as it is chemically inert and can retain its structural and morphological integrity under several conditions[18,22].

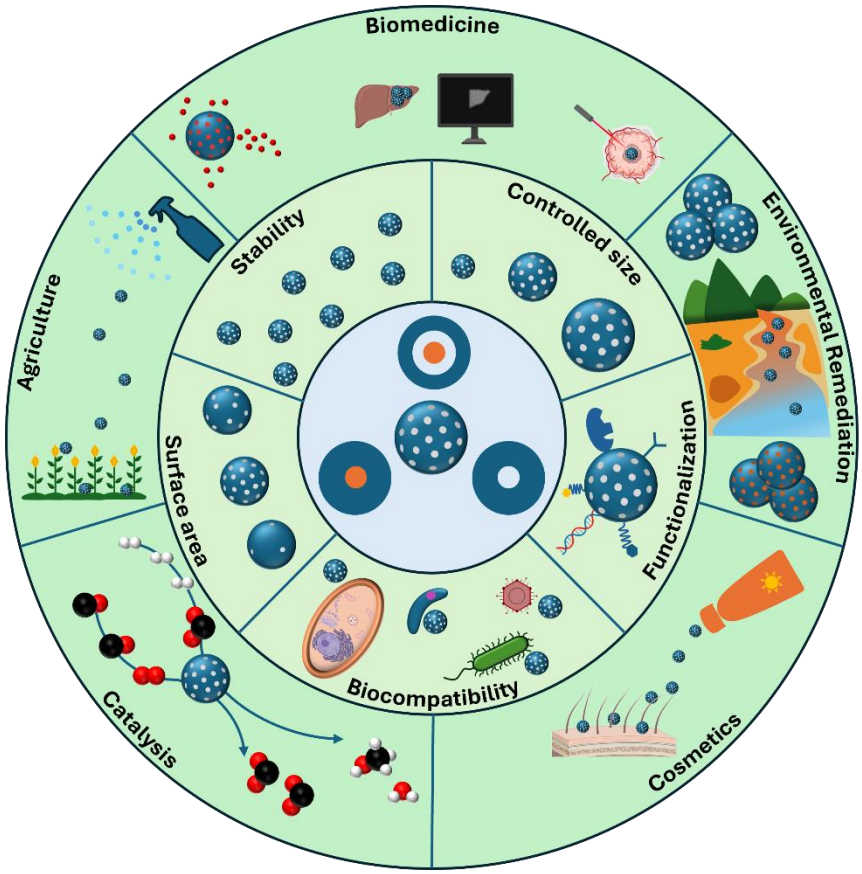

Figure 2 - Mesoporous silica nanoparticles. Possible core-shell structures, main properties and applications.

Indeed, adding to the properties referred above, silica shells are reported to stabilize the metal cores, prevent their aggregation, protect them from the surrounding medium, control the molecular or ion transport through the pores, and create novel structures with moldable properties[14,31]. These characteristics can be attributed to two main factors. First, the exposed silanol groups cause the accumulation of cations near silica surfaces, which, by turn, will generate long-range electrostatic repulsion forces between particles, resulting in better solubility in both water and even organic solvents and preventing aggregation. Then, due to its improved mechanical stability, mesoporous silica shells may be used to prevent morphological changes, a subject especially important during the alloying of bimetallic nanoparticles[14,32].

All these properties will be slightly changed according to the type of ordered mesostructured architecture that is a result of using different types of surfactant templates, consequently altering the pore symmetry, size, and volume[30]. The best-known arrangements

are Mobile Composition of Matter 41 (MCM-41) and Santa Barbara Amorphous 15 (SBA-15), both displaying a 2D hexagonal pore symmetry in the case of MCM-41 and SBA-15[28]. Usually, MCM-series exhibit pore sizes of around 2-5 nm and SBA-series have larger pore sizes of around 6-8 nm[33,34]. Additionally, there are the MSU-series, FDU-series, IBN-series, KIT-series, and several other[28,30,33].

1.2.1 Synthesis and characterization of Ag@MNs and alloys AgCu@MNs

Generally, there are two main strategies for nanoparticles synthesis. The top-down approach consists of breaking down the bulk material in order to obtain smaller particles, while the bottom-up approach is the opposite, starting with atoms or molecules and assembling them in a controlled way to obtain nanoparticles.[17,35] Typically, top-down relies on lithography and mechanical techniques while bottom-up opts more for chemical synthesis such as sol-gel synthesis and chemical vapor deposition.[17,18,35] None of these is properly better than the other, each has advantages and disadvantages that may suit better one particular type of nanoparticle. Briefly, top-down approach tends to be faster, although using great amounts of energy, while bottom-up enables better precision and complete control of the process. Since synthesizing core-shell nanoparticles requires a lot of control, bottom-up approaches have proven more appropriate.[18]

MNs are mainly synthesized by two methods: Stöber´s method and reverse micro emulsion. Both these methods are considered sol-gel methods with a surfactant-templating approach, once they require firstly a hydrolysis to generate free silanol groups and then the condensation between silanol groups around the micelle structure to form, after removing the template, the mesoporous silica structure.[27,30] The main difference between these methods it's that Stöber´s method is performed in water, ethanol, or a mixture of both, while reverse microemulsion is performed in water-in-oil (w/o) microemulsion where the silicate slowly diffuses into the nanodroplets of water that are dispersed in an organic solvent.[25,36] Other innovative methods include the swelling-shrinking mechanism and new modifications of the Stöber´s method in order to get a greener synthesis, using a surfactant-free synthesis through the pre-Ouzo effect.[37,38]

Typically, metal cores are synthesized by reducing the metal salts, but they can also be obtained by other chemical, physical, and even biological methods. In fact, over the last few years, green synthesis of metal nanoparticles has been highly requested once it allows to

reduce the organic compounds.[18,39] Briefly, the green synthesis uses natural extracts containing substances with reducing power that are present in living organisms to substitute the organic and inorganic reducing agents.[40,41]

Regarding chemical methods for the synthesis of AgNPs, they differ particularly in how the Ag^+ ions are reduced into Ag^0, being possible through a chemical reductant agent, photochemical, electrochemical, microwave-assisted, and sonochemical methods.[42] Furthermore, to obtain AgNPs there are essentially two stages: nucleation and growth. Nucleation happens when monomer concentration rises above the critical level of supersaturation, which triggers the "burst-nucleation" and precipitation. This generates the birth of new seeds and the dropping of the concentration below the critical level of supersaturation. Then, the monomers will be added to the seeds, promoting their growth.[42,43] For this purpose, both capping and reducing agents play a critical role in obtaining the desired nanoparticle.[44]

Moreover, when synthesizing bimetallic AgCuNPs, they can either end-up being in a core-shape structure if consecutively reductions are performed or they can present an alloy configuration if the reductions are performed simultaneously.[45] As such, when talking about bimetallic AgCu alloys, there are many methods that are capable of obtaining such particles with the most common consisting in a co-reduction process. This is a simple method that involves the mixture of both metal precursors (typically salts) and then, by adding a reducing agent to the solution, both will precipitate into bimetallic alloys.[45,46] Other methods include chemical precipitation, thermal decomposition, sol-gel, microemulsion, and hydrothermal.[45]

Then, after obtaining the metal cores, the most common method is by performing a template assisted sol-gel or microemulsion method to produce the silica shell.[14,47,48] Additionally, there are two ways of performing this. Either the core particles are synthesized separately and only then introduced in a solution that will coat the shell around it or the core nanoparticles are synthesized *in situ* and it is followed by the coating of the shell. The main advantage is that the first allows to obtain cores in a pure form, limiting the impurities on its surface, while the *in situ* synthesis is a simpler method that can in some cases enhance the interactions between core and shell.[18,48] The main difficulties of this method are the agglomeration of core particles in the reaction media, the incomplete coverage of the core surface and the formation of separate particles of shell material instead of coating the core nanoparticles.[18]

Finally, there are several characterization techniques available to analyze nanoparticles, each one according to which feature is expected to be characterized. The most important properties in a mesoporous core-shell nanoparticle are its morphology, topology, chemical, electrical and optical properties.[45]

Morphology must be completed using techniques such as Dynamic Light Scattering (DLS), Transmission Electron Microscopy (TEM), Scanning Electron Microscopy (SEM) and others, allowing to determine the size and shape of nanoparticles. On the other hand, topology is determined with the help of accessory instruments to TEM such as Energy Dispersive Spectrometry (EDS) that enables to characterize the chemical nature of the nanosystem and even produce an elemental mapping, as well as gas adsorption techniques like Brunauer-Emmett-Teller (BET), which determines the specific area of the porous structures.[47] Additionally, chemical and optical properties can be assessed using techniques like UV-Vis, Fourier Transform Infrared (FTIR) and Raman Spectroscopy, while electrical properties will be assessed by obtaining the zeta-potential.[45]

1.2.2 Metal core-shell MNs as Drug-delivery Systems

Drug delivery systems are described as drug formulations that can effectively deliver therapeutic agents to the active site. These systems can either be of immediate or controlled release. The main difference is that while the firsts typically release all or most of the drug in an initial burst without any control, a controlled drug delivery system releases the drug over a period of time, maintaining its concentration at the active site relatively constant.[49] Ideally, drug delivery systems should control both the release rate and for how long it happens as well as specifically directing it to a target site.[50]

The first nanoparticles to serve as drug-delivery systems were pegylated liposomes, but in the last few years MNs have been intensively studied due to its physicochemical features.[49,50] Indeed, silica-based nanoparticles present better stability and higher drug loading capacity compared to lipid nanoparticles and have already been approved by the US-FDA, recently entering clinical trials.[24,50] The BIOSCOPE Research Group has extensive experience in the synthesis of silica-based nanoparticles as drug delivery systems. These studies encompass several designs, ranging from simple MNS to core-shell MNs using gold, silver, platinum, palladium, superparamagnetic iron oxide (SPIONS) and even silicon quantum dots (QD) as cores. These drug-delivery systems show efficacy against both cancer cells and bacteria and some are even capable of producing stimuli-responsive mechanisms.[51–58]

Firstly, mesoporous silica presents a high pore volume that enables a high loading of drugs and a great variety, being able to carry and deliver from small molecules to macromolecules such as nucleic acids. Allied to the pore volume, the fact that it has a large surface area allows it to enhance the respective drug solubility, effectively carrying it to the targeted site. Moreover, its highly ordered structure delays the premature release of drugs and prevents their

degradation while its surface-active groups, namely silanol groups allow an easy functionalization process, being able to add more complexity to the system.[50,59,60]

Additionally, its tunable properties have a key role regarding drug-delivery systems. As interactions and dynamics between drug and system change from drug to drug, it is crucial that a system can adapt accordingly. Therefore, as MNs present tunable properties, it allows to modify its characteristics in order to better suit the respective drug being delivered. Also, studies show that toxicity of a determinate nanoparticle is highly dependent on features like shape, size, surface chemistry and charge. Thus, by adjusting these characteristics, it is possible not only to reduce toxicity, but also to improve other factors like biocompatibility, avoiding side effects and control biodistribution.[50,61]

Finally, due to functionalization processes, there are a great deal of possible modifications to improve the drug delivery-system. First, while passive targeting is possible, especially in cases of cancer, active targeting is a more specific targeting that involves ligands that selectively interact with the target cell or bacteria. For this kind of targeting, it is possible to chemically bind ligands to the silanol groups, which will thereafter improve bioavailability and minimize systemic toxicity.[18,50,59]

More than that, as silanol groups have such a variety of possible chemical bindings, it is even possible to perform a dual targeting, for example for the membrane cells and for an organelle such as mitochondria.[60] Moreover, it is also possible to use functional groups as gatekeepers in order to guarantee a sustained and controlled release only at the target site. Finally, smart polymers can be functionalized on the drug-delivery system surface, responding to exogenous or endogenous stimuli like pH, temperature, redox agents and others in order to release the drug only at the target site.[50,60,62]

In fact, the combination of metal core-shell MNs can be used exactly as a smart drug-delivery system. By combining both, not only silica will provide protection and stability to the metal core, but this last one will also play an important role in the drug-delivery system.[17,30] Metal cores can serve as a complementary approach both by acting as a secondary mechanism of treatment and by providing diagnostics, enabling the system to perform theranostics.[14,15] Briefly, metal cores can be used for imaging purposes, providing a diagnostic, act as a trigger for the release of the encapsulated drug or perform hyperthermia by plasmonic heating.[14,15,34,63]

Marcelo et al. engineered such a system, comprising a SPION core with a mesoporous silica shell functionalized with aliphatic chains that were subsequently cross-linked to SiQD probes. This system was made to address not only cancer cells, but also opportunistic bacterial

infections that appear during therapy. Thus, by loading it with two distinct drugs, one specific to cancer cells and the other specific to bacteria, they were able to produce a smart system with sustainable, biocompatible and biodegradable materials. Briefly, the release process was mediated by the SiQDs, that controlled pore access and allowed a higher release in pH 5 rather than pH 7.4, optimal for acute cancer environments. Moreover, the SPION core, due to its magnetic properties, allowed to perform hyperthermia treatment, which resulted in a higher release of both drugs and, therefore, an increased efficacy. Finally, although not entirely investigated, the fact that the SiQDs exhibit fluorescence might be a further application, as it can be used as imaging.[55]

This way, metal core-shell MNs are considered as a drug-delivery system with multifunctional properties that not only delivers the drug but stabilizes and takes the metal core to the site in a stealth and effective way, making it suitable for theranostics.

1.3 Antimicrobial Nanomaterials

In the last decades, due to the extensive use of antibiotics and lack of creating new ones, antibiotic-resistant microorganisms have had a rapid expansion, posing a global public health concern already expressed by the World Health Organization (WHO) and Centers for Disease Control and Prevention (CDC).[64,65] Indeed, approximately between 40-50% of surgery-related infections are caused by bacteria resistant to the conventional antibiotics and in the period of 1997 to 2006, the number of infections related to antibiotic-resistant bacteria increased by 359% in the USA.[66] For these reasons, in the last few years there have been incentives to develop novel and more effective antimicrobial compounds as well as reformulate and repurpose old antimicrobial agents.[64,66]

Recently, alongside antimicrobial resistance, WHO has alerted to the growing problem of sexually transmitted infections (STIs), registering more than one million cases daily worldwide.[67] Amongst the more than 30 distinct bacteria, viruses and parasites considered as sexual transmitted pathogens, there are eight accountable for the majority of STIs. From these, half are incurable viral infections, namely herpes simplex virus (HSV), hepatitis B, papillomavirus (HPV) and HIV, and the other half are curable caused by the protozoan parasite *Trichomonas vaginalis* and the bacteria *Chlamydia trachomatis*, *Treponema pallidum* and *Neisseria gonorrhoaea*.[68]

Nanomaterials have been intensely studied in the last years as a way to improve current antibiotics, both by serving as a drug-delivery system and by having an innate antimicrobial

effect.[69,70] Indeed, a wide range of nanomaterials have already been studied against STIs and reproductive tract infection (RTI), a wide term that involves STIs, referring more to the site of the infection rather than the way of transmission.[71,72] These systems allowed to improve vaginal retention with consequent increased drug permeation, also serving as a preventive and diagnostic tool in some cases.[71] Mesoporous silica, as already discussed, has been used with the purpose of improving drug delivery systems, but metal nanoparticles present special attention as most of them possess antimicrobial properties, being even described as a viable alternative to traditional antibiotics.[39,73]

The antimicrobial activity of metal nanoparticles is dependent on factors like their composition, surface area, and size. In general, their interaction with microorganisms triggers oxidative stress mechanisms, enzymatic inhibition and protein deactivation, changing the gene expression. Typically, its mechanisms involve oxidative stress, metal ion release, and non-oxidative mechanisms.[64]

Silver antimicrobial properties have been reported throughout human history. Indeed, AgNPs are the most studied antimicrobial agents, having antimicrobial activity against many bacteria, fungi, and viruses.[65,74] This intrinsic property, although not fully understood due to its complexity, is mainly caused by two processes: the dissolution and release of Ag^+ ions; and the reaction of AgNPs and Ag^+ ions with the cells themselves. These two factors will make possible the interactions between AgNPs/Ag^+ and the cell membrane, even being adsorbed on its surface. Only by being adsorbed, AgNPs can cause the production of reactive oxygen species (ROS) and when interacting with proteins such as ion channels can lead to their inactivation. Then, as smaller NPs and Ag^+ ions may enter the cell, both these processes will only continue and aggravate, destroying organelles and even DNA. All these mechanisms are described in Figure 3 and will lead to the cease of cell activity, disruption of its membrane and, eventually, its death.[44,75]

Similarly, although not in such highlight, CuNPs have also been extensively researched due to their properties. Indeed, their antimicrobial activity has been reported against many microorganisms while also being highly biocompatible.[73,76]

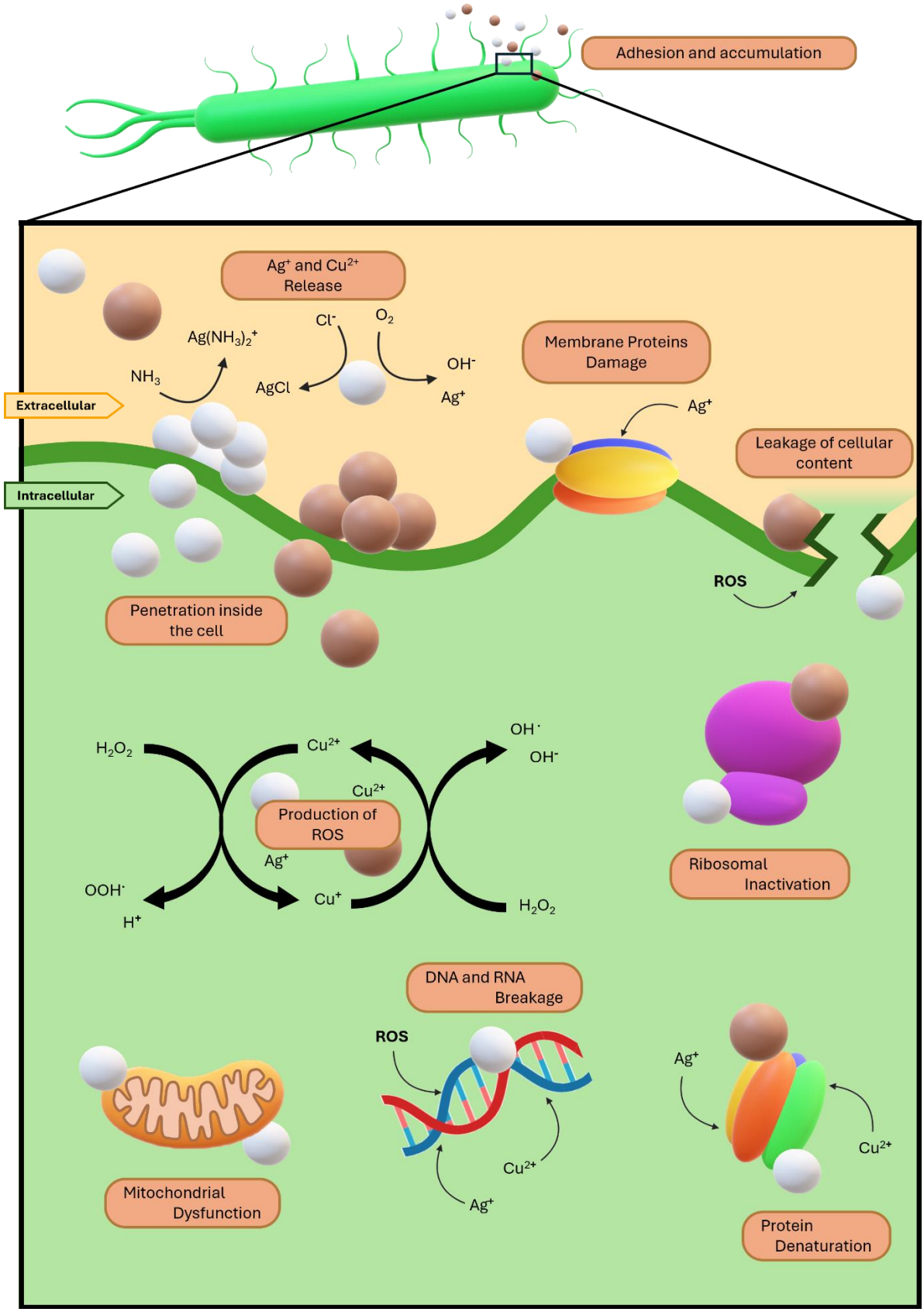

Figure 3 - AgNPs and CuNPs mechanisms of action against microorganisms.

Although the mode of action of CuNPs is not completely comprehended, some suggest that it might have resemblances to the mechanism of AgNPs, being depicted the main mechanisms in Figure 3. Indeed, both the dissolution and release of Cu^{2+} ions as well as the interactions of CuNPs/Cu^{2+} with the cells are of major importance.[76] As the superficial Cu atoms are oxidized, they originate Cu^{2+} ions, which will play a key role in this mechanism. Firstly, when CuNPs interact with the cell membrane, they can cause depolarization, inhibiting the mechanism of defense of some bacteria, the cell filament formation. Then, as Cu^{2+} ions are released into the medium, they will interact with the membrane, but will also be able to be uptake into cells. More than the fact that this will lead to the generation of ROS, it is also suggested that Cu^{2+} ions may have a high affinity to phosphorus and sulfur-containing biomolecules like DNA and proteins, leading to the structure distortion and consequently to the disruption of biochemical processes. All these combined will eventually lead to cell death.[77]

Finally, bimetallic nanoparticles formed by combining these two metals have already been investigated as they are important antimicrobial agents. One of the biggest issues when synthesizing AgNPs and CuNPs is their stability and the susceptibility of forming oxide species. Therefore, by combining them both, due to electronic attraction, it is possible to synthesize nanoparticles with higher stability and lower toxicity while also presenting synergistic properties. As such, the bimetallic AgCuNPs typically exceed the antimicrobial activity of either monometallic nanoparticle, reported to be more effective against Gram-positive bacteria rather than Gram-negative.[45,46,65,78–80]

1.3.1 Ag@MNs and AgCu@MNs as antimicrobial agents against *Candida albicans*

Alongside STIs, which their concern was highlighted in the 2023 WHO world congress, *Candida albicans* presents itself as the principal cause of Vulvovaginal candidiasis (VVC), one of the most common vaginal infections.[81] VVC is considered a RTI and is classified as a dysbiosis, which means a disruption in the vaginal microbiota balance. This is usually associated with genital inflammation, estimated to affect 40-45% of women worldwide twice or more times, with 5-9% experiencing recurrent VVC, defined as three or more infections per year.[82–85]

From *Candida spp*, *C. albicans* stands out as the most extensively researched species, playing a pivotal role as one of the most important agents of mucosal and systemic infections, being responsible for over 70% of all fungal infections worldwide. Moreover, it is considered

one of the most common life-threatening fungal species once, whenever it disseminated throughout the body, it leads to severe conditions, with a mortality rate of up to 40%.[86–88]

C. albicans also presents a threat to public health worldwide as its infection's occurrences have grown in the last two decades, getting more and more difficult to cure. Indeed, *Candida* species have the ability to form drug-resistant biofilms, which turns the disease more severe and harder to deal with.[89] Moreover, *C. albicans*, by causing a disruption in the vaginal microbiota balance, can be a risk factor for STIs.[90]

Metal nanomaterials, specifically silver and copper nanoparticles, have already been proved effective against these microorganisms. In fact, AgNPs have already been proved effective against multi-resistant strains of *N. gonorrhoeae*, not showing relevant cytotoxicity against mammalian cells and having synergetic effects with current ineffective antibiotics. This is highly important as is presents AgNPs both as bactericidal agents and potential adjuvants for available antibiotics.[91–95] Similarly, the efficacy of AgNPs against *C. albicans* has also been corroborated, not only inhibiting its growth, but leading to the death of the fungus, even showing enhanced activity compared to some conventional antifungal agents.[43,79,96]

Additionally, AgCu nanoalloys have been assessed against *C. albicans*, although the available literature on this subject is not extensive. Although some studies suggest that AgCuNPs only have inhibition properties, not been able to kill the fungus, there are several that prove its biocidal properties, mostly dependent on the intrinsic characteristics of the nanoparticles themselves. Nevertheless, in general, it is shown a synergistic effect of AgCuNPs against fungi, exhibiting better results that either AgNPs, CuNPs or even both monometallic nanoparticles mixed, therefore suggesting that the combination of the metals in a nanoalloy creates something not existent in both separately.[97–99] Finally, some articles prove that AgCuNPs can even exhibit stronger antifungal effects at lower concentrations that monometallic nanoparticles.[97–102]

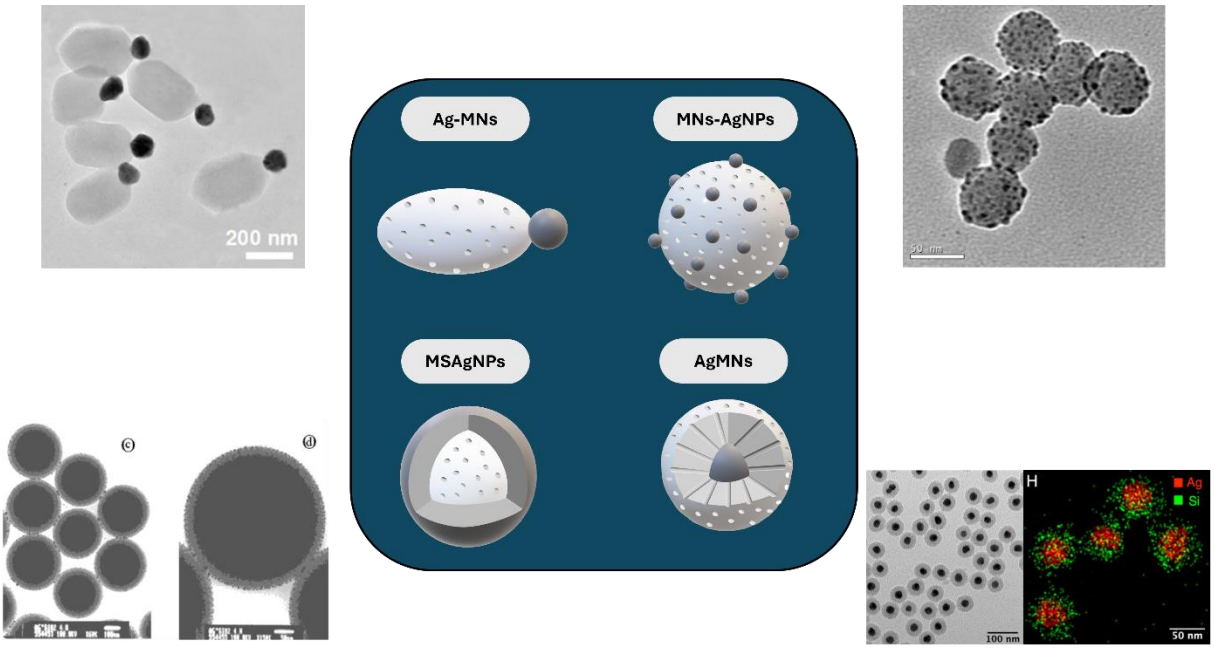

Figure 4 - Mesoporous silica and Silver nanoformulations. Ag-MNs: Janus like NPs. MNs-AgNPs: MNs coated with AgNPs; MSAgNPs: Mesoporous silica core with Ag shell NPs; AgMNs: Ag core with mesoporous silica shell. Adapted from [103–106].

Moreover, regarding nanomaterials against *C. albicans*, several nanosystems have been studied over the years, but indeed silver nanoparticles are highlighted, as they present significant antifungal activity and can even be conjugated with AMB, promoting a synergetic activity.[107] Even within silver nanormulations against *C. albicans*, there are several possible systems as seen in Figure 4 Nevertheless, when searching for nanosystems with Ag and SiO_2, it is more common to encounter articles that study MNs loaded with AgNPs on its pores and surface rather than a core shell Ag@MNs nanosystem.[105,108–110] Nevertheless, the MNs loaded with AgNPs exhibit promising results when tested against *C. albicans*. These kinds of systems were found to be very efficient, inhibiting biofilm formation and adhesion as well as decreasing the fungus viability and even successfully active against multi-drug-resistant strains.[105,108–110] Moreover, AgMNs have already been described as promising nanocarrier systems, as it decreases substantially the toxicity of silver and has the mesoporous structure, able to carry several types of drugs.[111]

To the best of our knowledge, despite its potential as described previously, there is no reported literature containing AgCu@MNs. Also, there are no reports on the impact of AgMNs on *C. albicans* and there is only one article reporting the conjugation of AMB in MNs.[112]

Table 1 - Summary of different Ag, Cu and SiO_2 based nanosystems used against desired microorganisms.

NP	Microorganism	Main conclusions	MIC (µg/mL)	AGAR dif. ø mm	Ref
AgNPs	*C. albicans*	Antifungal activity comparable to AMB	2.0	---	[113]
		AgNPs produced with peppermint extract have high efficacy	---	---	[114]
		Synergic effect with fluconazole	16	---	[115]
AgNPs / CuNPs	*C. albicans*	AgNPs have a higher effect than CuNPs	Ag - 50 Cu - 3200	---	[116]
		Submitting both NPs together has an effect comparable to AgNPs and superior to CuNPs	---	Ag - 18 Cu -15 Ag+Cu - 18	[100]
AgCuNPs	*C. albicans*	Ability to detach mature *C. albicans* biofilms	0.5 2.8	---	[101,102]
		Ability to inhibit its proliferation completely	0.78	---	[99]
		Ability to inhibit its growth after just 1 min	N.D	---	[117]
AgNPs / AgCuNPs	*C. albicans*	AgCuNPs are more effective than AgNPs	---	---	[98]
AgNPs / CuNPs / AgCuNPs	*C. albicans*	AgCuNPs are the most effective and showed antibiofilm activity	Ag - 12.5 Cu - 100 AgCu - 1.562	---	[118]
		AgCuNPs are the most effective	Ag - 250 Cu - 300 AgCu - 400	---	[119]
		AgCuNPs showed lower efficacy compared to AgNPs	Ag - 31 Cu - 250 AgCu - 62.5	Ag - 0.85 Cu - 1 AgCu - 0	[120]
		AgCuNPs showed lower efficacy compared to AgNPs	---	---	[121]
MNs-AgNPs	*C. albicans*	Antimicrobial activity comparable to AMB	1.0	---	[108]
	C. albicans *E. coli / S. aureus*	Significant antimicrobial activity, even at low concentrations	---	---	[109]

		Increased mechanical properties of PMMA matrix and antiadhesive effect	---	---	[110]
		Antimicrobial activity related to the production of ROS	6.0	---	[105]
		Long lasting antimicrobial activity	---	12	[122]
		Janus NPs have higher antibacterial activity than AgNPs	[40-80]	---	[104]
Ag-MNs	*C. albicans*	Kills up to 99.96% of the fungi within 18H	0.8	---	[123]
MSAgNPs	*S. mutans*	Lower antimicrobial activity than AgNPs, but better cytotoxicity	600	---	[124]
AgMNs	*E. coli / S. aureus*	Significant antibacterial and bactericidal effects, especially against Gram-negative bacteria	---	--	[125]
	E. coli / S. aureus	AgMNs have higher antibacterial effects than $AgTiO_2$	100	---	[126]
	E. coli / S. aureus B. cereus	Significant antibacterial effects	---	---	[127]
	S. enterica / E. coli /B. cereus	Significant bactericidal effects, especially against Gram-negative	[18.2-36.4]	---	[106]
	E. coli / S. aureus P. aeruginosa / …	Bactericidal efficacy is inversely proportional to the Ag core diameter and silica shell thickness	---	10	[128]
	A. naeslundii / E. faecalis / …	AgMNs possess longer antimicrobial activity than AgNPs	---	---	[129]
	K. pneumoniae / S. aureus / …	AgMNs show better efficacy than AgNPs	177	10	[130]
	C. albicans	AgMNs show strong antifungal activity	---	26.5	[131]
	---	Human endothelial cells take up high amounts of these nanosystems	---	---	[132]
SNPs-AMB	*C. albicans*	Highly efficient, long-lasting activity and do not exhibit significant cytotoxic effects	---	---	[133]
		Mainly efficient through contact	100	---	[134]
	---	Ability to load AMB into MNs and have a slow release for up to 56 days in Yeast Malt broth	---	---	[112]

Note - MNs-AgNPs: MNs coated with AgNPs; Ag-MNs: Janus like NPs. MSAgNPs: Mesoporous silica core with Ag shell NPs; AgMNs: Ag core with mesoporous silica shell. SNPs-AMB: Silica NPs functionalized with AMB.

2

OBJECTIVES

Following this introduction and understanding the benefits of creating a nanosystem that contains silver, copper and mesoporous silica, the present work has three main objectives. Firstly, it is aimed to synthesize AgCuMNs and properly characterize them. After this, these nanoparticles will be loaded with AMB and evaluate if it is able to be a nanocarrier. Finally, these nanosystems will be tested against one of the most important RTI (*C. albicans*) and will be assessed for its antifungal activity.

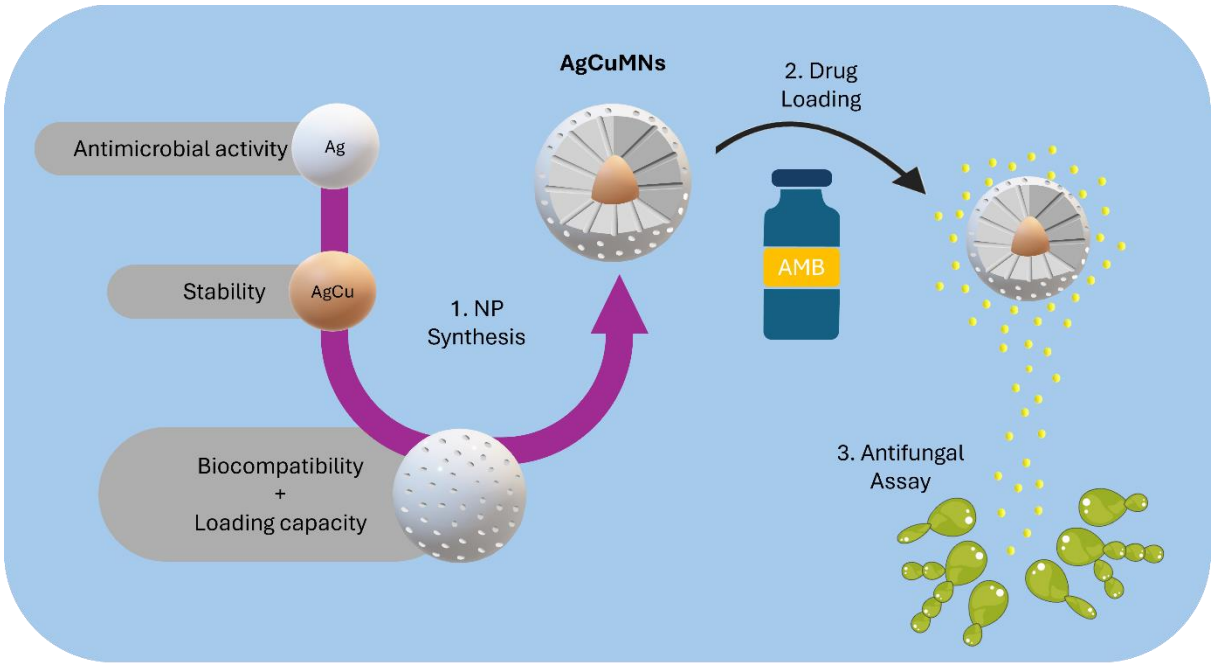

Figure 5 - General concept of the performed work with a schematic representation of the main objectives.

3

MATERIALS AND METHODS

3.1 Materials and Reagents

Ammonium nitrate (NH_4NO_3), hexadecyltrimethylammonium bromide (CTAB, ≥98%), sodium borohydride ($NaBH_4$, 99%), sodium citrate tribasic ($Na_3C_6H_5O_7$, 99%), and Amphotericin B trihydrate (AMB) were acquired from Sigma-Aldrich. Hydrogen peroxide (H_2O_2, 30%), potassium bromide (KBr, 99%), and sodium hydroxide (NaOH) were purchased from PanReac AppliChem, while Dimethyl sulfoxide (DMSO), ethanol (EtOH), and methanol (MeOH) were bought from Honeywell. Sabouraud Dextrose Agar (SDA) and Muller Hinton Broth (MHB) were acquired from Biokar diagnostics, silver nitrate ($AgNO_3$, 99%) was from Alfa Aesar and ethylene glycol (EG) was bought from CarloErba. Tetraethyl orthosilicate (TEOS, 99.9%) was purchased from thermoscientific. All reagents were used as bought and all solutions were prepared in deionized MilliQ H_2O unless otherwise indicated.

Also, due to its importance as a RTI and one of the main causes for vaginal infections, *Candida albicans* (Robin) Berkhout (ATCC$^{(R)}$ 10231^{TM}) was selected to study the antifungal properties of the selected nanomaterials.

3.2 Instrumentation

UV-vis absorption spectra were acquired on a Jasco V-650 spectrophotometer (Jasco Corporation, Tokyo, Japan) and Infrared spectra (FTIR) were collected on an Alpha II (Bruker, Massachusetts, USA). Nanoparticle size distributions and zeta potential were measured using a dynamic light scattering (DLS) Malvern Nano Zetasizer, with a 633 nm laser diode, from PROTEOMASS–BIOSCOPE Research Group facility (Caparica, Portugal). AMB concentration (both at

loading and release) was determined using a Nanodrop 1000 Spectrophotometer (ThermoFisher). Antifungal assays were conducted in asepsis guaranteed by a laminar flux chamber Steril-VBH. Sterile flat-bottom transparent 96-well plates were from Greiner Bio-One (Dreieich-Buchschlag, Germany). Incubations were executed in a Mermmet Incubator B10 and the reading of the plates was conducted in a UV-Vis CLARIOstar spectrophotometer (BMG Labtech).

3.3 Synthesis of mesoporous silica-based nanoparticles

3.3.1 Synthesis of mesoporous silica nanoparticles (MNs)

The synthesis of mesoporous silica nanoparticles (MNs) was achieved according to Galhano et al.[57] First off, 150 mg of CTAB ($CH_3(CH_2)_{15}N(Br)(CH_3)_3$) were dissolved in 30 mL of MilliQ H_2O and left stirring for 30 min at 50 ºC under smooth agitation. Then, it was added to the solution 10 mL of ethylene glycol, 700 µL of a 1M NaOH aqueous solution, and 750 µL of TEOS drop by drop, leaving the resulting mixture under stirring for 3 hours at 80 ºC.

Finally, having obtained MNs, it was only necessary a template removal step. With this purpose, a procedure of Zhang et al.[135] was followed, which consisted of suspending the nanoparticles in a 30 mg/mL ammonium nitrate solution in methanol and leaving it stirring for 1 hour at 60 ºC, being washed thrice with methanol. This procedure was repeated, ending up by leaving the clean MNs to dry at room temperature (r.t.).

3.3.2 Synthesis of silver mesoporous silica nanoparticles (AgMNs)

The synthesis of silver mesoporous silica nanoparticles (AgMNs) was performed in two consecutive steps. Firstly, spherical AgNPs were synthesized by the method proposed by Frank et al.[136] Briefly, it was successively added in a round bottom flask freshly prepared 2 mL of a solution 1.25×10^{-2} M of sodium citrate, 5 mL of a solution 3.75×10^{-4} M of silver nitrate, 5 mL of a solution 5×10^{-2} M of hydrogen peroxide, 40 µL of a solution 1×10^{-3} M of potassium bromide, and 2.5 mL of a solution5 5×10^{-3} M sodium borohydride in MilliQ H_2O. After having all solutions in the flask, it was carefully stirred for approximately 3 min at room temperature.

After obtaining AgNPs, the formation of a mesoporous silica shell was performed according to Nuti et al.[58] Briefly, 30 mL of MilliQ H_2O was added to the AgNPs previous solution, followed by the addition of 150 mg of CTAB, and, after being left under stirring for 30 min at

50 ºC, it was added to the solution 10 mL of ethylene glycol, 700 µL of a 1M NaOH aqueous solution, and 750 µL of TEOS drop by drop, leaving the resulting mixture under stirring for 3 hours at 80 ºC. Finally, having obtained AgMNs, the same template removal protocol was performed on MNs.

3.3.3 Synthesis of silver-copper mesoporous silica nanoparticles (AgCuMNs)

The synthesis of silver-copper mesoporous silica nanoparticles, in similarity with AgMNs was achieved in two consecutive steps: synthesizing AgCu cores and their encapsulation in a mesoporous silica shell. AgCu cores were provided by the PROTEOMASS-BIOSCOPE Research Group. Then, a similar protocol used to obtain AgMNs was carried out for 1mL of AgCu cores suspension.

3.4 Nanoparticles characterization

After their synthesis, it was important to properly characterize the nanoparticles, determining their size, stability, pore size distribution, and others. With this purpose, five different characterization techniques were used: absorption spectroscopy; FTIR; DLS; TEM; and N_2 adsorption/desorption isotherms.

Absorption spectroscopy was used to characterize AgNPs, specifically its shape. This is only possible due to previous reports where a correlation between maximum absorption peak and shape was determined.[136] Therefore, it was performed a simple dilution of the obtained AgNPs suspension with MilliQ H_2O, which were respectively measured in the spectrophotometer, using a quartz cuvette.

Moreover, all mesoporous silica-based nanoparticles (MNs, AgMNs, and AgCuMNs) were characterized by FTIR spectroscopy in order to study its surface chemistry and by N_2 adsorption/desorption isotherms to understand its pore size distribution. FTIR spectrum was obtained with Alpha II equipment. N_2 adsorption/desorption isotherms were obtained with the help of Chemistry Department of FCT NOVA, where the samples were sent to and properly analyzed in order to determine the surface area and pore size distribution. For this, Brunauer Emmett and Teller (BET) and Barrett-Joyner-Halenda (BJH) methods were used.

Finally, all nanoparticles were characterized by DLS and TEM, allowing to be determine both their hydrodynamic diameter, but also their true diameter without solvent interactions, as well as its shape, polydispersity and zeta-potential. DLS measurements were conducted by

dispersing the nanoparticles into MilliQ H_2O in low concentrations and then introducing it onto a glass cuvette, which was respectively put onto the equipment. For obtaining the zeta potential, a dip cell was introduced into the same glass cuvette and followed the analysis. TEM images were obtained with the help of INL - International Iberian Nanotechnology Laboratory, where the samples were sent to and properly analyzed.

3.5 Loading trials

Amphotericin B was the drug used to be encapsulated in mesoporous silica-based NPs due to its use against *C. albicans* infections. For the loading assay, 40 mg of the respective nanoparticle (MNs, AgMNs or AgCuMNs) were suspended in 2 mL of DMSO with a concentration of 0.5 mg/mL of AMB. The mixture was placed under stirring in a dark environment at room temperature for 24 hours.

After 24h, the mixtures were centrifuged (5 000 RPM, 5 minutes) and washed with MilliQ H_2O solution twice. After collecting all the supernatants, it was acquired the UV-vis spectra of each one and applied the Lambert-Beer Law in order to quantify the amount of drug in the supernatant. The molar absorptivity coefficient (ε) was calculated by previously performing a calibration curve for AMB, obtaining the value of 7835.5 $M^{-1}cm^{-1}$ in DMSO at 416 nm.

Loading capacity (mg/g) and loading efficiency (%E) were determined by UV-vis spectroscopic quantification and mass balances by the equations presented below.

t_{drug} - total amount of drug; f_{drug} – amount of free drug present on the supernatant.

$$\%E = \frac{t_{drug} - f_{drug}}{t_{drug}} \times 100 \qquad loading\ capacity\ \left(\frac{mg}{g}\right) = \frac{t_{drug} - f_{drug}}{amount\ of\ nanoparticles}$$

3.6 Antifungal assays

All nanomaterials tested and the AMB solution with the corresponding concentration loaded in each nanoparticle were made in DMSO. Nanoparticles suspensions had a concentration of 8 mg/mL.

C. albicans strain stock was kept at -80 ºC in broth with glycerol (15% v/v). In the first step of the antifungal assay, *C. albicans* was subcultured on Sabouraud Dextrose Agar (SDA) plates and left incubating for approximately 36 hours at 30 ºC.

So, after the incubation period, isolated colonies were transferred from the SDA plates to a saline medium (NaCl 0.85% m/v). The turbidity of the suspensions was adjusted to 0.5 on the McFarland scale (about 10^6 CFU/mL) and subsequently diluted 10-fold, leading to an approximately final suspension of 10^5 CFU/mL. For each sample, 20 µL were added to the first well of the 96-well plate, performing a series of successive dilutions, which obtained a gradient concentration with a range of 800 - 1.6 µg/mL. Finally, 10 µL of *C. albicans* suspension previously prepared (10^5 CFU/mL) was added to each well, leaving the plates to incubate for roughly 28 hours at 30 ºC.

After this period, an aliquot of each well was sub-cultured on the surface of SDA plates, leaving them to incubate for over 66 hours at 30 ºC. The Minimum Fungicidal Concentration (MFC) was then determined by naked-eye assessment of the SDA plates though a drop plates assay.

Simultaneously, optical density (OD) measurements of the 96-well plates turbidity were quantified using a UV-Vis CLARIOstar spectrophotometer (BMG Labtech) at 600 nm. *C. albicans* viability was calculated by comparing the sample OD_{600} with the control OD_{600}. Though this method, it was possible to determine the Minimum Inhibitory Concentration (MIC).

Free AMB and unloaded MNs, AgMNs, and AgCuMNs were used as controls for the experiment, *C. albicans* incubated in the absence of any nanomaterial or drug was used as a negative control, and nanomaterials and AMB incubated without *C. albicans* were used as controls. Each sample was tested in duplicate, and two independent experiments were performed.

4

Results and Discussion

4.1 Synthesis and Characterization of Metal core-shell silica nanoparticles

Metal Ag cores were synthesized by the Frank Method, where the reagents used were sodium citrate, silver nitrate, hydrogen peroxide, potassium bromide, and sodium borohydride. Firstly, all these reagents were put into a round flask, without any steering, and in the order described previously. Then, by gently steering it, the reaction occurred, forming the desired nanoparticles.

In the reaction itself, silver nitrate served as the source of silver ions, while sodium borohydride was responsible to reduce the Ag^+ ions to Ag^0 atoms, which resulted in forming AgNPs. Both potassium bromide and sodium citrate were in high concentrations, the first controlling the nanoparticle size, ensuring the desired shape, while sodium citrate acted as both a buffer and stabilizer by associating with Ag^+ ions on the nanoparticle surface, preventing aggregation. Finally, hydrogen peroxide played a complementary role to sodium borohydride, acting as an etching agent. This way, it removed newly formed, less stable AgNPs, allowing only the least reactive NPs to persist and grow at the expense of more reactive ones. This way, it creates a balance between the formation of new nanoparticles and the removal of undesired ones, ensuring a homogeneous solution containing the desired AgNPs.[136–138]

On this process, two main details proved to be crucial to obtain the desired nanoparticles. Firstly, both the fact that all solutions were freshly prepared, including the MilliQ H_2O, and that new flasks were used, guaranteeing the avoidance of contaminations was extremely important. This is because any contamination in the flasks may affect the synthesis, for example by serving as an undesired nucleation seed, or by oxidizing the AgNPs, since they are extremely sensible to oxidation.[139,140]

Due to the optical characteristics of AgNPs, the colorimetric alteration of the solution allows us to evaluate whether the reaction occurred as intended or not. Initially, all reagent solutions are transparent, and even after combining them in the round flask, the mixture remains clear. However, after gently stirring for approximately 2 minutes, a sudden color change occurs, with the solution turning dark black. It then gradually brightens, transitioning to vivid yellow for round-shaped AgNPs and dark blue for triangular-shaped AgNPs. Figure 6 (A) shows how the AgNPs presented themselves to the naked eye at the end of the reaction and Figure 6 (B) is the respective absorption spectra, presenting two distinct spectra. This way, as reported by Frank et all, we obtained successfully round yellow AgNPs with a peak at 419 nm and triangular blue AgNPs with a peak at 748 nm, which are contained in the ranges reported for each nanoparticle.[136]

Mesoporous silica nanoparticles (MNs) and silica shell on silver and silver-copper core-shell silica nanoparticles (AgMNs and AgCuMNs) were performed by a modified Stöber method, a sol-gel method. Firstly, as a cationic surfactant, CTAB was dissolved in water in order to arrange itself in hexagonal cylinder micelles and, therefore, serve as template for the pores of the nanoparticles. Then, after well-dissolved, Ethylene glycol, sodium hydroxide and TEOS were added to the mixture. Ethylene glycol served as the stabilizing agent by reducing the surface tension between micelles, which is essential to prevent their aggregation and assure their dispersion through the solution, therefore producing monodispersed nanoparticles with similar structure and size. Sodium hydroxide, by favoring an alkaline environment, will work as both the catalyst and the morphological agent, as a basic pH leads to the hydrolysis of the silica precursor, TEOS, and then its precipitation onto the cationic templates. After the proper amount of time for the reaction to occur, the desired nanoparticles are obtained.

After this, it is vital to remove the template because, firstly, the surfactant would impede the incorporation of any other molecule on the NPs pores and, secondly, the surfactant itself presents intrinsic toxicity, what would influence the antifungal results.[141] So, with this purpose, and recognizing the increased difficulty in removing templates of MCM-41 silica nanoparticles prepared under basic media due to its stronger interactions between the surfactant and the silica framework, an ammonium nitrate solution in methanol was used.[142] This method performs a solvent extraction by ion exchange without altering the size nor the uniformity of the pores and keeping the Si-OH groups.

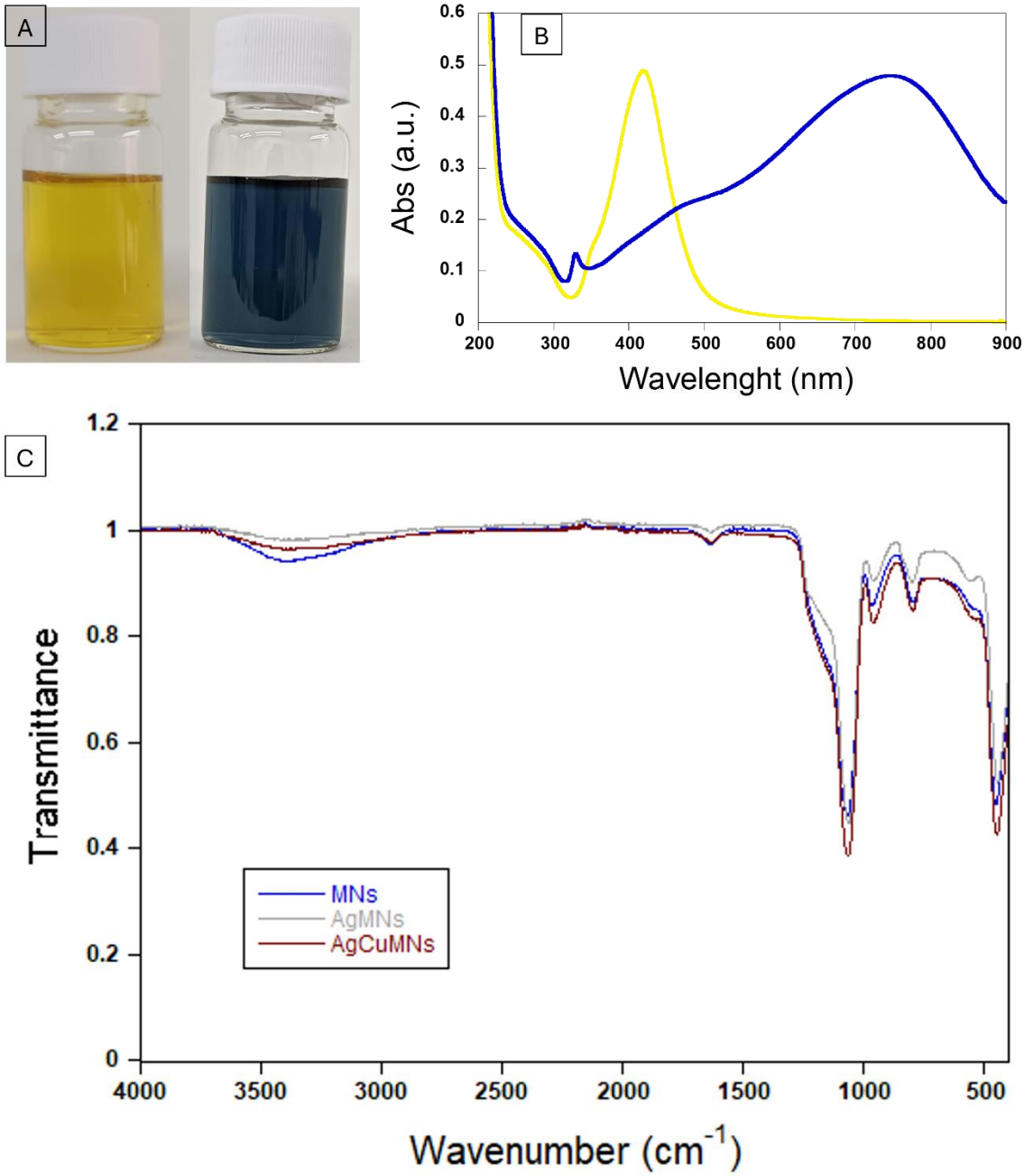

Figure 6 - AgNPs: round (yellow) and triangular (blue) shaped. (A) naked eye solutions and (B) respective absorption spectra. (C) FTIR spectra of MNS, AgMNs, and AgCuMNs after the template removal process.

The template removal process effectiveness can be confirmed by FTIR.[143] Figure 6 (C) shows the FTIR spectra of MNs, AgMNs and AgCuMNs after removing the template of these nanoparticles and, by analyzing it, it is clear that all three show a similar aspect. Furthermore, there are two main details that we can delve into. Firstly, it is clearly seen the peaks particular to mesoporous silica, such as at 1075 cm^{-1} and 970 cm^{-1}, which are characteristic of Si-O-Si and

Si-O-H vibrations, respectively. The peak at 800 cm^{-1} also adds to this group, representing Si-O-Si symmetric stretching vibrations. Then, if any CTAB remained at the end of the template removal process, two specific peaks, 2919 cm^{-1} and 2835 cm^{-1}, would have appeared. The absence of these peaks in our spectra proves that the template removal process was successful, therefore obtaining NPs without any CTAB.[143–145]

After verifying the complete removal of surfactant from our nanoparticles, the AgCu alloys, AgMNs and AgCuMNs were sent to further study, at INL, to be analyzed by TEM. The corresponding pictures are in Figure 7 (A, B, and C), with the respective data regarding its sizes in the graphs of Figure 7 (D, E, and F). First, it is important to note that we were able to synthesize AgCu nanoalloys with a narrow size dispersion, sizing around 5 nm. Then, regarding both core-shell nanoparticles, AgMNs and AgCuMNs, were both successfully produced. Nevertheless, there are a few aspects that will need future improvements. Upon close examination of Figure 7 (C), we observe that, although we can indeed spot some core-shell AgMNs, there are also simple MNs lacking a silver core. By contrast, analysis of Figure 7 (B) reveals that while some AgCu cores were correctly encapsulated within a mesoporous silica shell, the covering was incomplete, leaving some AgCu nanoalloys dispersed without any shell. Finally, comparing these nanoparticles, it is interesting to notice that both AgMNs and AgCuMNs have a similar size, around 50 nm, with an almost identical size distribution.

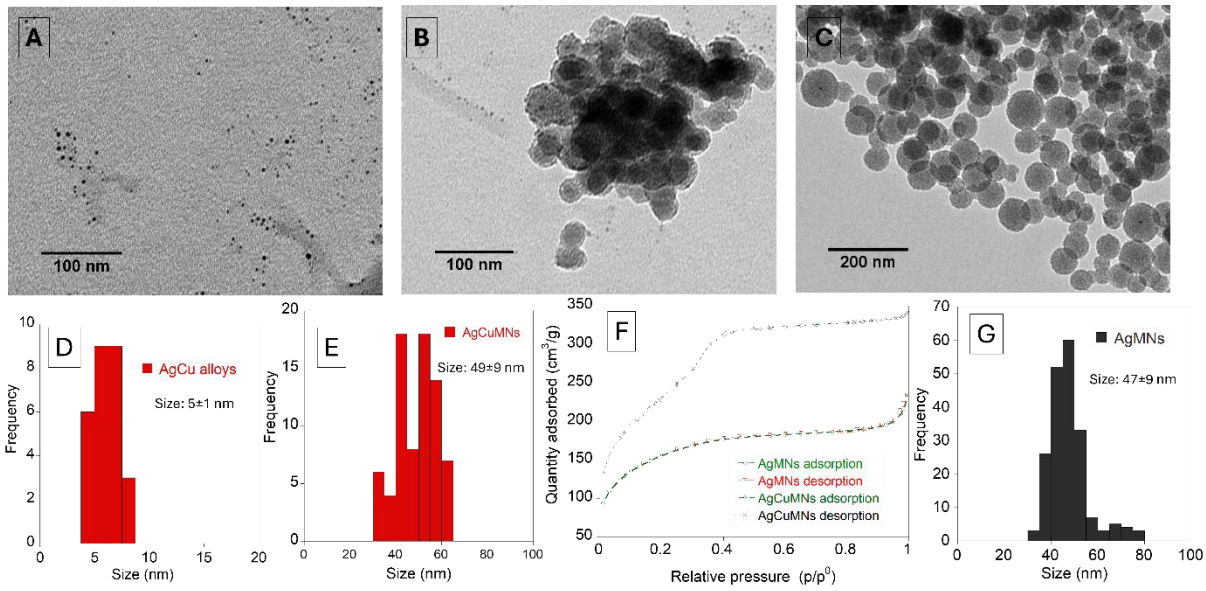

Figure 7 - TEM Images of AgCu Alloys (A), AgCuMNs (B) and AgMNs (C). (D, E, G) Size histograms and Nitrogen isotherms (F) of the synthesized nanoparticles.

Besides their real size, the hydrodynamic size of these several nanoparticles was also measured as well as their Polydispersity index (PDI) and zeta-potential (Table 2). Firstly, it is

evident that all mesoporous silica-based NPs have a higher hydrodynamic size than the metal nanoparticles as well as much higher than their real size measured by TEM. This was expected, as not only these nanoparticles use the metal nanoparticles as cores, excluding MNs, but also due to the presence of Si-OH groups, which interact with H_2O molecules, increasing its solvation sphere and, consequently, its hydrodynamic diameter.[146,147] Moreover, in similarity to what was obtained by Nuti et al., AgNPs exhibit a zeta-potential lower than -30.0 mV, which indicates its colloidal stability.[58] Finally, comparing all mesoporous silica-based NPs, it is noted that while MNs are similar to AgCuMNs, AgMNs present some disparity. Indeed, AgMNs present the smallest hydrodynamic diameter and a neutral zeta-potential in MilliQ H_2O, which is according to what was seen experimentally, once AgMNs were more prone to aggregate in H_2O compared to MNs and AgCuMNs.

Table 2 - DLS data of all nanoparticles synthesized performed in H_2O: Hydrodynamic diameter (dH), Polydispersity Index (PDI), and Zeta-potential (ζ).

NP	dH (nm)	PDI	ζ (mV)
Ag	46 ± 3	0.388 ± 0.048	-37.3 ± 5.1
MNs	919 ± 114	0.739 ± 0.140	-12.4 ± 0.2
AgMNs	658 ± 72	0.588 ± 0.112	0.5 ± 0.1
AgCuMNs	938 ± 240	0.853 ± 0.089	-13.0 ± 0.7

Finally, the last characterization test performed was the N_2 adsorption/desorption isotherms. AgMNs and AgCuMNs were the only nanoparticles tested, as this method allows to determine the surface area, the pore volume, and the pore size though their adsorption and desorption of N_2 at different pressures. Its histograms can be seen in Figure 7 (F) and the resulting measurements in Table 3.

Regarding the porosity of AgMNs and AgCuMNs, firstly, by analyzing Figure 7 (F), we can identify that, although slightly different, both samples display a type IV isotherm. This, in accordance with the TEM images, confirms both particles present a mesoporous arrangement, since this type of curve is characteristic of ordered mesoporous materials.[148,149] Furthermore, from these curves, it was used the BET method to calculate the surface area as well as the pore size, while the pore volume was calculated by the BJH method. So, by looking at Table 3, we can conclude that although AgCuMNs present both a higher surface area as well as pore volume compared with AgMNs, both nanoparticles have similar pore sizes, which are within the normal range for MCM-41 type NPs (2-10 nm). [148,150] Nonetheless, even though that both

AgMNs and AgCuMNs present an ordered mesoporous structure, their surface area is lower than the usual values for MCM-41 MNs.[151] This might have other factors, but one that can be easily identified is that, by both nanoparticles processing a metal core, it is natural that their surface area is lower as the core does not have pores on its inside.

Table 3 - BET and BJH porosimetry measurements for AgMNs and AgCuMNs nanoparticles

	AgMNs	AgCuMNs
Surface area		
BET Surface Area	562.4425 m^2/g	837.6045 m^2/g
BJH Adsorption cumulative surface area of pores between 1.7000 nm and 300.0000 nm width	258.7573 m^2/g	639.5487 m^2/g
BJH Desorption cumulative surface area of pores between 1.7000 nm and 300.0000 nm width	227.7318 m^2/g	607.4919 m^2/g
Pore volume		
BJH Adsorption cumulative volume of pores between 1.7000 nm and 300.0000 nm width	0.227726 cm^3/g	0.419758 cm^3/g
BJH Desorption cumulative volume of pores between 1.7000 nm and 300.0000 nm width	0.212334 cm^3/g	0.404987 cm^3/g
Pore size		
Adsorption average pore diameter (BET)	2.5803 nm	2.5185 nm
BJH Adsorption average pore diameter	3.5203 nm	2.6253 nm
BJH Desorption average pore diameter	3.7296 nm	2.6666 nm

4.2 Loading of Amphotericin B

Amphotericin B is a drug that has low solubility in aqueous environments and low permeability through biological membranes, being categorized by the Biopharmaceutics Classification System (BCS) as a class IV drug. As demonstrated in Figure 8 (A) it has both hydrophilic groups such as the hydrophilic tail and the polyol chain, and also hydrophobic ones such as the polyene chain, therefore possessing amphipathic properties. Moreover, it is also considered an amphoteric molecule due to the carboxylic acid and the mycosamine sugar.[152] Due to these properties, biomembranes and its constituents, namely, sterols like ergosterol, are the primary target of AMB, creating transmembrane pores that allow ions to pass through, consequently disturbing the cell electrostatics. Although not fully understood, some articles point out that

AMB has two main modes of activity towards *C. albicans*. These consist in binding during the budding stage to young cells' membranes, affecting its structural properties and physiological ion transport and by penetrating into the cytoplasm, interfering in physiological processes.[153]

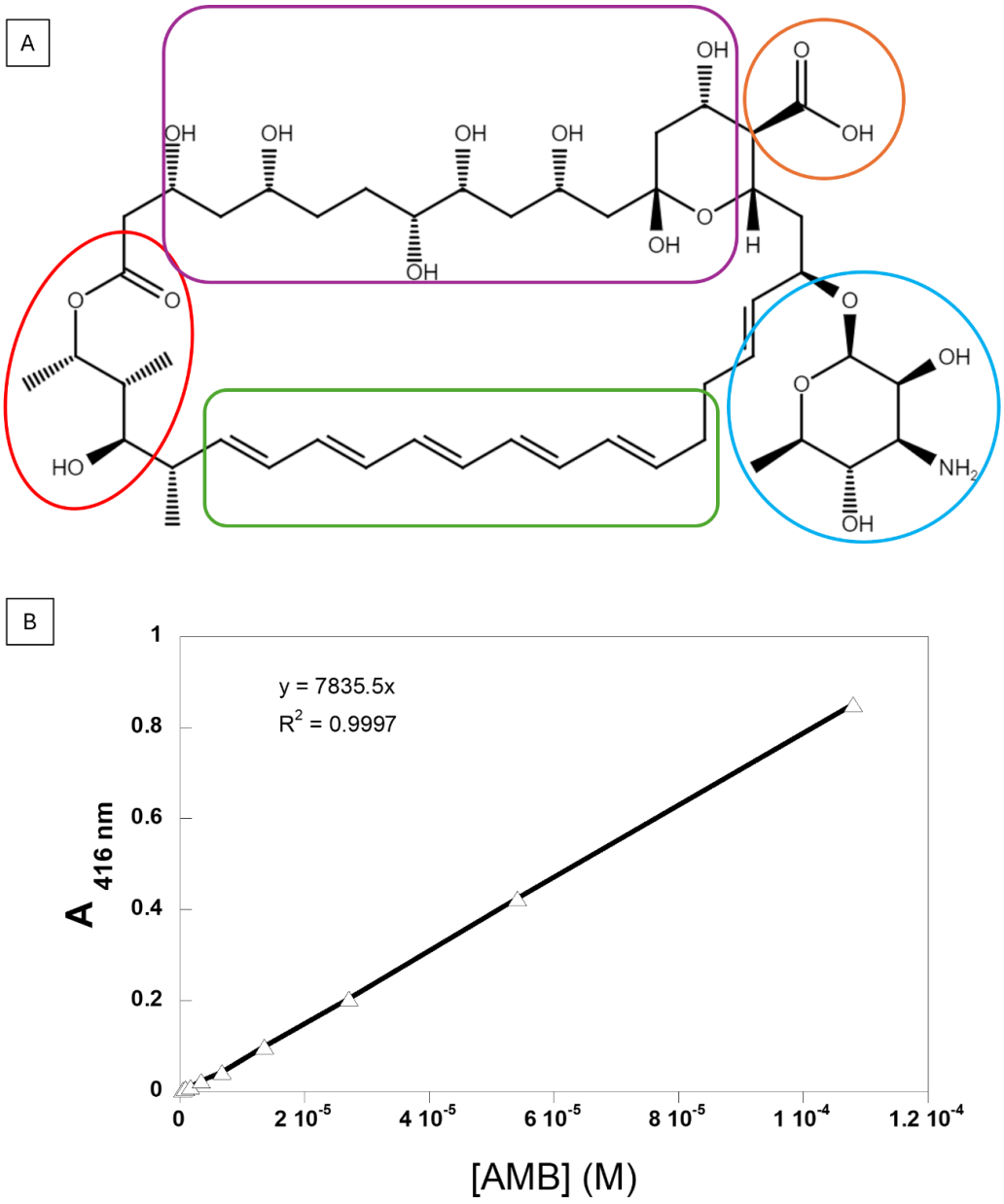

Figure 8 - Amphotericin B (AMB) chemical structure and main groups (A): red - Hydrophilic tail; green - Polyene chain; blue - Mycosamine sugar; orange - carboxylic acid; purple - Polyol chain. And (B) molar absorptivity coefficient (ε) in DMSO calibration curve.

Therefore, due to its poor water solubility, the ε was determined in DMSO, obtaining the result of 7835.5 $M^{-1}cm^{-1}$. This value was determined by successive dilutions, acquiring all the respective absorption spectra.

Following this step along with the synthesis of the nanoparticles, the loading of AMB was performed in each one of the nanomaterials: MNs, AgMNs, and AgCuMNs. This reaction occurred in a dark environment because AMB reportedly suffers photo-degradation when exposed to light.[154,155] Furthermore, the choice of solvent was a crucial step since it was critical to perform the loading process in a solvent were both AMB and nanomaterials are soluble. So, being DMSO one of the few solvents where AMB is highly soluble, while also dissolving the nanoparticles, this was the selected one.[152,156] Then, after completing the loading, it was also important to determine which solvent to use in the washing process. This step must be performed with a solvent soluble to the nanoparticles, but not to AMB, so that it keeps most of the drug encapsulated. The solvent used was MilliQ H_2O.

Table 4 - Loading percentage and Encapsulation efficacies for loaded nanomaterials.

	MNs	**AgMNs**	**AgCuMNs**
Loading (%)	90.4	93.5	90.1
EE ($\mu g_{drug}/mg_{NP}$)	14.50	14.75	14.62

After completing the loading process, the resulting supernatants from the washing step were analyzed and the corresponding absorption spectra was acquired. Then, by using the calibration curve previously determined (Figure 8 (B)), the loading percentage and encapsulation efficacies were calculated, being presented in Table 4. In general, all nanomaterials had a significantly high percentage of loading, corroborating the idea that mesoporous silica is an ideal carrier for drugs. Furthermore, it is to be noted that the loading percentages were very similar, proving the reproducibility of this method and making comparable nanomaterials for further studies.

Lee et al. also encapsulated AMB into MNs, though using a different method. Indeed, they incorporated MNs into a PMMA matrix and immersed the resulting disk specimens into 2 mL solution of AMB in DMSO. This resulted into a low percentage of loading (7.2%).[112] Thereby, we conclude that our loading process of solubilize the MNs into a liquid solution instead of dispersing them into a solid matrix contributes significantly to obtain higher percentages of loading.

4.3 Antifungal assays

After characterizing all nanomaterials, it was assessed their antifungal and fungicidal properties against *C. albicans*, as it is one of the main causes of vaginal infections and presents itself as an important RTI. To perform this assay, 96-well plates were used for a broth microdilution assay, followed by the determination of the minimum fungicidal concentration (MFC) using SDA plates, and ending it with OD_{600} measurements.

This enabled the determination of the minimum inhibitory concentration (MIC) and the MFC for each nanomaterial. In this work, the MIC represents the nanoparticle concentration at which there is a 50% decrease in the microorganism growth, and the MFC as the nanoparticle concentration at which, after the transfer from the 96-well plate to the SDA plate, it is verified no growth. These parameters serve as indicators for the nanomaterial's antifungal activity, allowing a comparative analysis between them.

For these assays, the samples tested were all the nanoparticles previously characterized (MNs, AgMNs and AgCuMNs) both loaded with AMB and free, as well as free AMB. All samples were dispersed in DMSO, and nanoparticles were dispersed into 8 mg/mL solutions. Since the loading percentages were similar between all nanoparticles, it was only necessary to prepare one solution of free AMB corresponding to the concentration encapsulated into the nanoparticles. Therefore, considering Table 4, an AMB solution was prepared with a final concentration of 0.12 mg/mL.

In order to determine which concentration range should be used in the assay, it is first important to note that the AMB MIC values for *C. albicans* are not consensual throughout literature. This is expected once this parameter depends heavily on the strain used, the type of assay performed, and even on the drug itself.[157,158] Therefore, after careful research across literature, it was understood that most of MIC values were contained in a range from 8 to 0.1 µg/mL.[159–168] Taking this into account, the broth microdilution assay was performed using a nanomaterial concentration range from 800 to 1.56 µg/mL, which, in the loaded nanoparticles, corresponds to a range of AMB encapsulated from 12 to 0.023 µg/mL.

Figure 9 displays the graphics that correlate the fungal growth with the sample concentration, allowing us to analyze the outcomes from the broth microdilution assay after OD_{600} measurements. Table 5 summarizes the MICs obtained during this assay and the MFCs obtained by the drop plates assay. The analysis of both sources allows for a comprehensive evaluation of the data acquired.

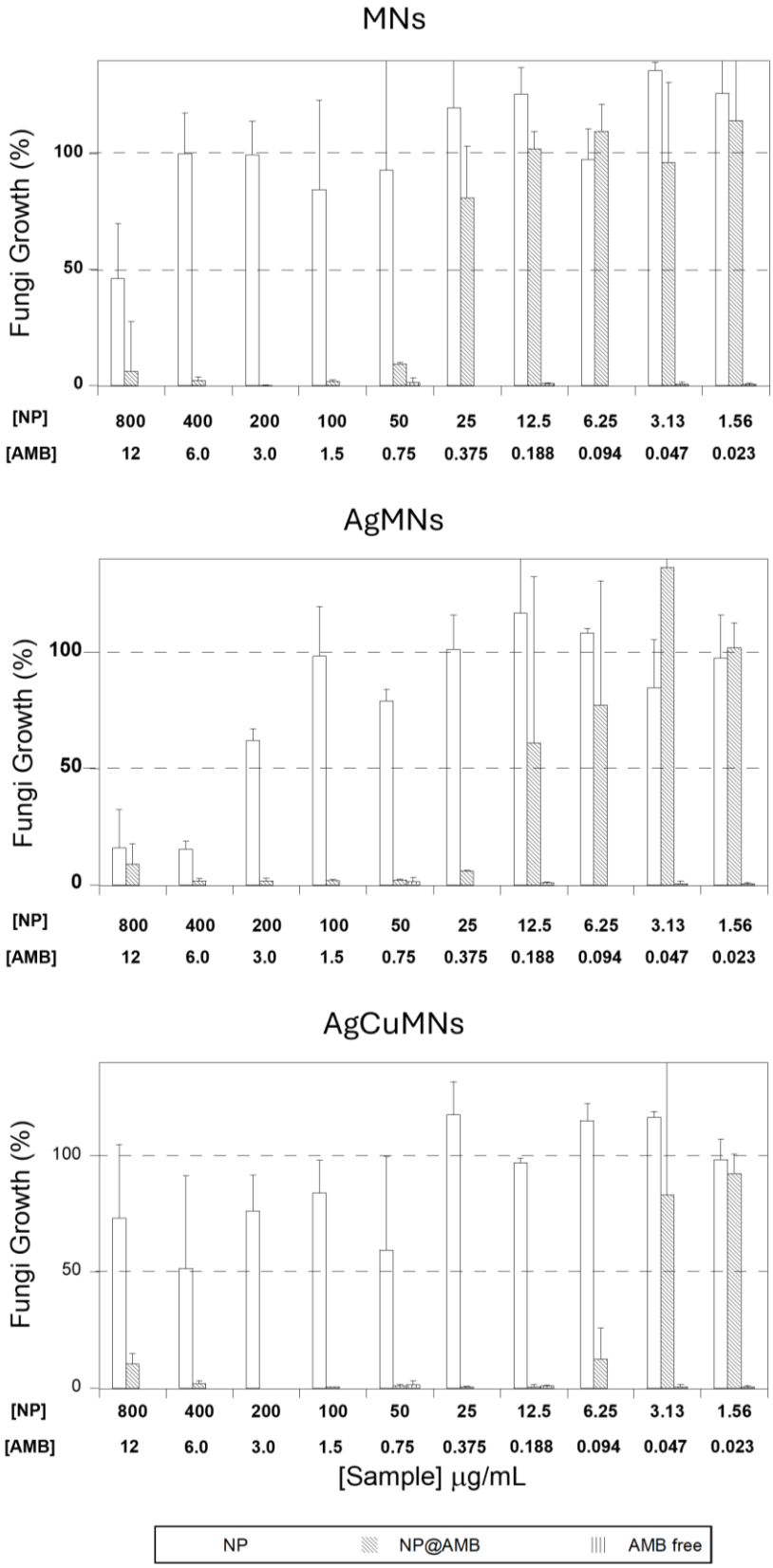

Figure 9 - Inhibitory activity, as fungi growth (%), of (*from top to bottom*) MNs, AgMNs, and AgCuMNs, against *C. albicans*. For each sample, it was tested only the nanoparticle free (NP), loaded with AMB (NP@AMB), and the respective AMB concentration without NP (AMB free).

First and foremost, it must be highlighted that, by successfully encapsulating AMB into our mesoporous silica-based NPs, we were able to produce a system that significantly improves the solubility of AMB. Indeed, one of the main issues associated with this drug is its poor solubility in aqueous media, which hinders their pharmacological applications.[169,170] Our mesoporous silica-based nanosystems were able to be dispersed in aqueous media, therefore proving themselves as efficient nanocarriers for this drug.

Secondly, no nanoformulation was able to produce the same effect as free AMB, thus not being verified a potentiation between the drug and the nanomaterial. This aspect may be attributed to several reasons, namely the poor solubility of AMB in aqueous media. Indeed, even though *C. albicans* might sometimes slightly acidify the pH of the medium, MHB is an aqueous medium with a reported pH of 7.4 ± 0.2.[171–173] So, in accordance with all this, it was also expected that AMB would not be easily released from the nanoparticles. Moreover, AMB is also reported to form aggregates in aqueous media, but as recommended, it was first dissolved in DMSO, thus being solubilized.[174] Accordingly, we suspect that it interacted with the fungi as intended, leading to such a high effectiveness. Therefore, we estimate that AMB may be well encapsulated into the mesoporous silica matrix, tending to stay like that instead of being dispersed into a solvent where it is poorly solubilized.

Then, even though the release of the drug might have been limited, it is clear that all loaded nanoparticles were much more effective against *C. albicans* compared to the same nanoparticles unloaded. This is understandable through the MIC evaluation where both MNs and AgMNs had a 16-fold diminution, 800 to 50 µg/mL and 400 to 25 µg/mL, respectively, but was even more pronounced in AgCuMNs. The MIC of these nanoparticles unloaded was not detected, but the loaded ones had a MIC of 6.25 µg/mL of nanoparticles, which corresponds to an AMB concentration of 0.089 µg/mL. Furthermore, the MFC results also corroborate this statement as no free nanoparticle was able to fully produce fungicidal effects, but all loaded nanoparticles exhibited MFCs in the range of 400 to 200 µg/mL of nanoparticles, corresponding to AMB concentrations of 6.00 and 3.00 µg/mL.

Table 5 - Minimum Inhibitory Concentration (MIC) and Minimum Fungicidal Concentration (MFC) for each sample against *C. albicans*.

Sample ID	MIC (µg/mL)		MFC (µg/mL)	
	[NP]	[AMB]	[NP]	[AMB]
MNs	800	-	ND	-
MNs@AMB	50	0.64	400	6.00
AgMNs	400	-	ND	-
AgMNs@AMB	25	0.35	400	6.00
AgCuMNs	ND	-	ND	-
AgCuMNs@AMB	6.25	0.089	200	3.00
AMB_{free}	-	<0.023	-	0.047

Therefore, from all the nanoformulations tested, AgCuMNs@AMB were the most effective ones against *C. albicans*. Indeed, although AgCuMNs may not produce as strong antifungal effects as AgMNs, as shown by their non-detected MIC compared to the 400 µg/mL MIC for AgMNs, when loaded with AMB, the AgCuMNs@AMB exhibit a MIC of 6.25 µg/mL. This is four times lower than the MIC of AgMNs@AMB, which is 25 µg/mL. Although we are not certain of the exact reason, from what is described in the literature, the conjugation of Cu with Ag may produce a system more stable and, therefore, that is oxidized gradually over time.[175–177] We suspect that this effect produces a prolonged action, which seems to have a synergetic effect when conjugated with AMB and, therefore, a more pronounced effect onto *C. albicans*.

Finally, in order to evaluate the potential of AgCuMNs as a nanocarrier, it must be compared with the typical AMB administration. Generally, AMB is administered intravenously due to its poor absorption in the gastrointestinal tract and the solutions generally prescribed contain concentrations between 0.2 and 2 mg/mL.[178–180] Our results showed that our system can not only improve the solubility of the drug, but also produce fungicidal effects in concentrations almost 1 000 times lower than the ones used in current medicine. Hence, we can verify the effectiveness of AgCuMNs as drug-delivery systems and their future potential.

5

CONCLUSIONS

This work had the focus of combining silver, copper, and mesoporous silica into a nanosystem. The main objectives were to produce, load, and test this type of nanosystems against infectious diseases, namely *C. albicans*. Now, reaching its end, we can state that all three of these aims were successfully achieved.

Firstly, both Ag and AgCu cores were obtained, with AgCu nanoalloys being about 5 nm diameter. Then, both these cores were successfully encapsulated within a mesoporous silica shell, obtaining AgMNs and AgCuMNs. Both these nanoparticles had a size around 50 nm diameter, reaching a much higher hydrodynamic size due to the interaction of silanol groups with water molecules. Then, by analyzing the TEM images, it was understood that while some AgMNs had no Ag core, therefore presenting themselves simply as MNs, AgCuMNs showed some AgCu nanoalloys not encapsulated, therefore indicating some issue with the encapsulating process. Nevertheless, both nanoparticles displayed pore sizes and surface area values consistent with those typical of MCM-41 MNs, though the surface areas were lower due to their metal core. So, we can conclude that both AgMNs and especially AgCuMNs were successfully synthesized, allowing us to proceed with our planned work.

After this, the MNs, AgMNs, and AgCuMNs were loaded with AMB, obtaining loading percentages of around 90% for all three of them. This is highly important since it proves three particular aspects. First, by obtaining such high loading percentages, we can understand the effectiveness of our method, especially when compared with other solid matrix methods. Then, by achieving similar percentages within all three nanosystems, although this method should be confirmed with other drugs and nanomaterials, our results suggest that it may be

reproducible. Finally, with this step, by increasing significantly the solubility of AMB in aqueous systems, we corroborate the theory that mesoporous silica may be ideal as a drug carrier.

Regarding the last objective, all three nanoformulations were then tested against *C. albicans* in a broth microdilution assay, which allowed us to draw several conclusions. First and foremost, it is important to note that, even with the mesoporous shell confining the silver cores, the AgMNs had still an antifungal effect. Then, all three nanosystems had a stronger effect on *C. albicans* when loaded with AMB compared to the unloaded ones. From the three nanoparticles, AgCuMNs showed the highest difference between unloaded and loaded, going from no MIC detected, to a MIC of 6.25 µg/mL of AgCuMNs@AMB, which corresponds to an AMB concentration of 0.089 µg/mL. AgCuMNs@AMB was indeed the most effective nanoformulation, presenting a potential synergy of AgCu nanoalloys with the AMB drug and proving itself as a potential drug delivery system.

Considering the presented work, it displays the initial steps of a promising class of drug delivery systems that may play a critical role in the fight against infectious diseases. The subsequent work would consist of improving the encapsulating process in order to have homogeneous samples with all core-shell nanoparticles and determine its efficiency. It would also be important to repeat the loading method with other antimicrobiotics that target other infectious diseases in order to guarantee its reproducibility, as well as further studies on the AgCu - AMB interactions, to better understand the observable synergetic effect. Finally, it would be a major step if we could analyze how does our nanosystem work under more realistic infection scenario, for example with *ex vivo* tests. This way, we could acknowledge whether it significantly improves the today common medical practices, if it may be used to fight the growth of *C. albicans* infections and as a tool to stop the spread of antibiotic-resistant microbes.

6
BIBLIOGRAPHY

1. Bayda, S., Adeel, M., Tuccinardi, T., Cordani, M. & Rizzolio, F. The History of Nanoscience and Nanotechnology: From Chemical–Physical Applications to Nanomedicine. *Molecules* **25**, 112 (2019).
2. Malik, S., Muhammad, K. & Waheed, Y. Nanotechnology: A Revolution in Modern Industry. *Molecules* vol. 28 Preprint at https://doi.org/10.3390/molecules28020661 (2023).
3. Moungi G. Bawendi, L. E. B. and A. Y. The Noble Prize in Chemistry. *The Noble Prize* https://www.nobelprize.org/prizes/chemistry/ (2023).
4. Jun, B.-H. *Nanotechnology for Bioapplications*. vol. 1309 (Springer Singapore, Singapore, 2021).
5. Leon, L., Chung, E. J. & Rinaldi, C. A brief history of nanotechnology and introduction to nanoparticles for biomedical applications. in *Nanoparticles for Biomedical Applications* 1–4 (Elsevier, 2020). doi:10.1016/B978-0-12-816662-8.00001-1.
6. Contera, S., De La Serna, J. B. & Tetley, T. D. Biotechnology, nanotechnology and medicine. *Emerging Topics in Life Sciences* vol. 4 551–554 Preprint at https://doi.org/10.1042/ETLS20200350 (2021).
7. nano. https://www.dictionary.com/browse/nano (2023).
8. Zhang, L., Liu, T., Xie, Y., Zeng, Z. & Chen, J. A new classification method of nanotechnology for design integration in biomaterials. *Nanotechnol Rev* **9**, 820–832 (2020).
9. Patel, K. D., Singh, R. K. & Kim, H.-W. Carbon-based nanomaterials as an emerging platform for theranostics. *Mater Horiz* **6**, 434–469 (2019).
10. Kumar, S. *et al.* Optically Active Nanomaterials and Its Biosensing Applications—A Review. *Biosensors (Basel)* **13**, 85 (2023).
11. Sengul, A. B. & Asmatulu, E. Toxicity of metal and metal oxide nanoparticles: a review. *Environ Chem Lett* **18**, 1659–1683 (2020).

12. El-Toni, A. M. *et al.* Design, synthesis and applications of core–shell, hollow core, and nanorattle multifunctional nanostructures. *Nanoscale* **8**, 2510–2531 (2016).
13. Singh, R. & Bhateria, R. Core–shell nanostructures: a simplest two-component system with enhanced properties and multiple applications. *Environ Geochem Health* **43**, 2459–2482 (2021).
14. Hanske, C., Sanz-Ortiz, M. N. & Liz-Marzán, L. M. Silica-Coated Plasmonic Metal Nanoparticles in Action. *Advanced Materials* **30**, (2018).
15. Su, H. *et al.* Nanoporous core@shell particles: Design, preparation, applications in bioadsorption and biocatalysis. *Nano Today* **31**, 100834 (2020).
16. Wei, S. *et al.* Multifunctional composite core–shell nanoparticles. *Nanoscale* **3**, 4474 (2011).
17. Tsamos, D., Krestou, A., Papagiannaki, M. & Maropoulos, S. An Overview of the Production of Magnetic Core-Shell Nanoparticles and Their Biomedical Applications. *Metals (Basel)* **12**, 605 (2022).
18. Ghosh Chaudhuri, R. & Paria, S. Core/Shell Nanoparticles: Classes, Properties, Synthesis Mechanisms, Characterization, and Applications. *Chem Rev* **112**, 2373–2433 (2012).
19. Nalluri, S. R., Nagarjuna, R., Patra, D., Ganesan, R. & Balaji, G. Large Scale Solid-state Synthesis of Catalytically Active Fe3O4@M (M = Au, Ag and Au-Ag alloy) Core-shell Nanostructures. *Sci Rep* **9**, 6603 (2019).
20. He, Q., Zhang, Z., Xiong, J., Xiong, Y. & Xiao, H. A novel biomaterial — Fe3O4:TiO2 core-shell nano particle with magnetic performance and high visible light photocatalytic activity. *Opt Mater (Amst)* **31**, 380–384 (2008).
21. Zhang, Q., Lee, I., Joo, J. B., Zaera, F. & Yin, Y. Core–Shell Nanostructured Catalysts. *Acc Chem Res* **46**, 1816–1824 (2013).
22. Gao, C., Lyu, F. & Yin, Y. Encapsulated Metal Nanoparticles for Catalysis. *Chem Rev* **121**, 834–881 (2021).
23. Pajor-Świerzy, A., Szczepanowicz, K., Kamyshny, A. & Magdassi, S. Metallic core-shell nanoparticles for conductive coatings and printing. *Adv Colloid Interface Sci* **299**, 102578 (2022).
24. Kankala, R. K., Han, Y.-H., Xia, H.-Y., Wang, S.-B. & Chen, A.-Z. Nanoarchitectured prototypes of mesoporous silica nanoparticles for innovative biomedical applications. *J Nanobiotechnology* **20**, 126 (2022).
25. Huang, Y. *et al.* Silica nanoparticles: Biomedical applications and toxicity. *Biomedicine & Pharmacotherapy* **151**, 113053 (2022).

26. Akhter, F. *et al.* A Comprehensive Review of Synthesis, Applications and Future Prospects for Silica Nanoparticles (SNPs). *Silicon* **14**, 8295–8310 (2022).
27. Jeelani, P. G., Mulay, P., Venkat, R. & Ramalingam, C. Multifaceted Application of Silica Nanoparticles. A Review. *Silicon* **12**, 1337–1354 (2020).
28. Maleki, A. *et al.* Mesoporous silica materials: From physico-chemical properties to enhanced dissolution of poorly water-soluble drugs. *Journal of Controlled Release* **262**, 329–347 (2017).
29. Croissant, J. G., Fatieiev, Y., Almalik, A. & Khashab, N. M. Mesoporous Silica and Organosilica Nanoparticles: Physical Chemistry, Biosafety, Delivery Strategies, and Biomedical Applications. *Adv Healthc Mater* **7**, (2018).
30. Kankala, R. K. *et al.* Nanoarchitectured Structure and Surface Biofunctionality of Mesoporous Silica Nanoparticles. *Advanced Materials* **32**, (2020).
31. He, X. *et al.* Silver Mesoporous Silica Nanoparticles: Fabrication to Combination Therapies for Cancer and Infection. *The Chemical Record* **22**, (2022).
32. Albrecht, W., van der Hoeven, J. E. S., Deng, T.-S., de Jongh, P. E. & van Blaaderen, A. Fully alloyed metal nanorods with highly tunable properties. *Nanoscale* **9**, 2845–2851 (2017).
33. Popat, A. *et al.* Mesoporous silica nanoparticles for bioadsorption, enzyme immobilisation, and delivery carriers. *Nanoscale* **3**, 2801 (2011).
34. Li, Z., Zhang, Y. & Feng, N. Mesoporous silica nanoparticles: synthesis, classification, drug loading, pharmacokinetics, biocompatibility, and application in drug delivery. *Expert Opin Drug Deliv* **16**, 219–237 (2019).
35. Baig, N., Kammakakam, I. & Falath, W. Nanomaterials: a review of synthesis methods, properties, recent progress, and challenges. *Mater Adv* **2**, 1821–1871 (2021).
36. Wu, S.-H., Mou, C.-Y. & Lin, H.-P. Synthesis of mesoporous silica nanoparticles. *Chem Soc Rev* **42**, 3862 (2013).
37. Narayan, R., Nayak, U., Raichur, A. & Garg, S. Mesoporous Silica Nanoparticles: A Comprehensive Review on Synthesis and Recent Advances. *Pharmaceutics* **10**, 118 (2018).
38. Chen, Z. *et al.* A non-surfactant self-templating strategy for mesoporous silica nanospheres: beyond the Stöber method. *Nanoscale* **12**, 3657–3662 (2020).
39. Camacho-Jiménez, L., Álvarez-Sánchez, A. R. & Mejía-Ruíz, C. H. Silver nanoparticles (AgNPs) as antimicrobials in marine shrimp farming: A review. *Aquac Rep* **18**, 100512 (2020).

40. Asmathunisha, N. & Kathiresan, K. A review on biosynthesis of nanoparticles by marine organisms. *Colloids Surf B Biointerfaces* **103**, 283–287 (2013).
41. Rani, P. *et al.* Highly stable AgNPs prepared via a novel green approach for catalytic and photocatalytic removal of biological and non-biological pollutants. *Environ Int* **143**, 105924 (2020).
42. Xu, L. *et al.* Silver nanoparticles: Synthesis, medical applications and biosafety. *Theranostics* **10**, 8996–9031 (2020).
43. Zhang, X.-F., Liu, Z.-G., Shen, W. & Gurunathan, S. Silver Nanoparticles: Synthesis, Characterization, Properties, Applications, and Therapeutic Approaches. *Int J Mol Sci* **17**, 1534 (2016).
44. Lee, S. & Jun, B.-H. Silver Nanoparticles: Synthesis and Application for Nanomedicine. *Int J Mol Sci* **20**, 865 (2019).
45. Idris, D. S. & Roy, A. Synthesis of Bimetallic Nanoparticles and Applications—An Updated Review. *Crystals (Basel)* **13**, 637 (2023).
46. Zain, N. M., Stapley, A. G. F. & Shama, G. Green synthesis of silver and copper nanoparticles using ascorbic acid and chitosan for antimicrobial applications. *Carbohydr Polym* **112**, 195–202 (2014).
47. Gawande, M. B. *et al.* Core–shell nanoparticles: synthesis and applications in catalysis and electrocatalysis. *Chem Soc Rev* **44**, 7540–7590 (2015).
48. Chen, Q., Ge, Y., Granbohm, H. & Hannula, S.-P. Effect of Ethanol on Ag@Mesoporous Silica Formation by In Situ Modified Stöber Method. *Nanomaterials* **8**, 362 (2018).
49. Park, H., Otte, A. & Park, K. Evolution of drug delivery systems: From 1950 to 2020 and beyond. *Journal of Controlled Release* **342**, 53–65 (2022).
50. Ahmed, H. *et al.* Biomedical applications of mesoporous silica nanoparticles as a drug delivery carrier. *J Drug Deliv Sci Technol* **76**, 103729 (2022).
51. Fernández-Lodeiro, A. *et al.* Synthesis of Mesoporous Silica Coated Gold Nanorods Loaded with Methylene Blue and Its Potentials in Antibacterial Applications. *Nanomaterials* **11**, 1338 (2021).
52. Marcelo, G. A. *et al.* Luminescent silicon-based nanocarrier for drug delivery in colorectal cancer cells. *Dyes and Pigments* **181**, 108393 (2020).
53. Marcelo, G. A., Duarte, M. P. & Oliveira, E. Gold@mesoporous silica nanocarriers for the effective delivery of antibiotics and by-passing of β-lactam resistance. *SN Appl Sci* **2**, 1354 (2020).

54. Marcelo, G. A. *et al.* Development of New Targeted Nanotherapy Combined with Magneto-Fluorescent Nanoparticles against Colorectal Cancer. *Int J Mol Sci* **24**, 6612 (2023).
55. Marcelo, G. A. *et al.* Magneto-Fluorescent Mesoporous Nanocarriers for the Dual-Delivery of Ofloxacin and Doxorubicin to Tackle Opportunistic Bacterial Infections in Colorectal Cancer. *Int J Mol Sci* **23**, 12287 (2022).
56. Marcelo, G. *et al.* Toxicological Evaluation of Luminescent Silica Nanoparticles as New Drug Nanocarriers in Different Cancer Cell Lines. *Materials* **11**, 1310 (2018).
57. Galhano, J., Marcelo, G. A., Duarte, M. P. & Oliveira, E. Ofloxacin@Doxorubicin-Epirubicin functionalized MCM-41 mesoporous silica–based nanocarriers as synergistic drug delivery tools for cancer related bacterial infections. *Bioorg Chem* **118**, 105470 (2022).
58. Nuti, S. *et al.* Engineered Nanostructured Materials for Ofloxacin Delivery. *Front Chem* **6**, (2018).
59. Vallet-Regí, M., Schüth, F., Lozano, D., Colilla, M. & Manzano, M. Engineering mesoporous silica nanoparticles for drug delivery: where are we after two decades? *Chem Soc Rev* **51**, 5365–5451 (2022).
60. Vallet-Regí, M., Colilla, M., Izquierdo-Barba, I. & Manzano, M. Mesoporous Silica Nanoparticles for Drug Delivery: Current Insights. *Molecules* **23**, 47 (2017).
61. Mohan, A., Santhamoorthy, M. & Lee, Y.-C. Recent advances in the pH-responsive organic–inorganic mesoporous hybrid silica for targeted drug delivery. *Eur Polym J* **206**, 112783 (2024).
62. Song, Y., Li, Y., Xu, Q. & Liu, Z. Mesoporous silica nanoparticles for stimuli-responsive controlled drug delivery: advances, challenges, and outlook. *Int J Nanomedicine* **Volume 12**, 87–110 (2016).
63. Wen, J. *et al.* Diverse gatekeepers for mesoporous silica nanoparticle based drug delivery systems. *Chem Soc Rev* **46**, 6024–6045 (2017).
64. Baptista, P. V. *et al.* Nano-Strategies to Fight Multidrug Resistant Bacteria—"A Battle of the Titans". *Front Microbiol* **9**, (2018).
65. Bakina, O. *et al.* Design and Preparation of Silver–Copper Nanoalloys for Antibacterial Applications. *J Clust Sci* **32**, 779–786 (2021).
66. Yan, J. *et al.* Chemical Synthesis of Innovative Silver Nanohybrids with Synergistically Improved Antimicrobial Properties. *Int J Nanomedicine* **Volume 18**, 2295–2305 (2023).
67. Abisoye-Ogunniyan, A. *et al.* A Survey of Preclinical Studies Evaluating Nanoparticle-Based Vaccines Against Non-Viral Sexually Transmitted Infections. *Frontiers in Pharmacology* vol. 12 Preprint at https://doi.org/10.3389/fphar.2021.768461 (2021).

68. Sexually transmitted infections (STIs). https://www.who.int/news-room/fact-sheets/detail/sexually-transmitted-infections-(stis) (2023).
69. Unemo, M., Golparian, D. & Eyre, D. W. Antimicrobial Resistance in Neisseria gonorrhoeae and Treatment of Gonorrhea. in *Methods in Molecular Biology* vol. 1997 37–58 (Humana Press Inc., 2019).
70. Terreni, M., Taccani, M. & Pregnolato, M. New antibiotics for multidrug-resistant bacterial strains: Latest research developments and future perspectives. *Molecules* vol. 26 Preprint at https://doi.org/10.3390/molecules26092671 (2021).
71. Chindamo, G., Sapino, S., Peira, E., Chirio, D. & Gallarate, M. Recent advances in nanosystems and strategies for vaginal delivery of antimicrobials. *Nanomaterials* **11**, 1–29 (2021).
72. Khan, Z. *et al.* Evaluation of reliability of self-collected vaginal swabs over physician-collected samples for diagnosis of bacterial vaginosis, candidiasis and trichomoniasis, in a resource-limited setting: a cross-sectional study in India. *BMJ Open* **9**, e025013 (2019).
73. El-Shenawy, F. A., El-Sherbeny, E. M. El. & Kassem, S. Efficacy of zinc oxide and copper oxide nanoparticles on virulence genes of avian pathogenic E. coli (APEC) in broilers. *BMC Vet Res* **19**, 108 (2023).
74. Nqakala, Z. B. *et al.* Advances in Nanotechnology towards Development of Silver Nanoparticle-Based Wound-Healing Agents. *Int J Mol Sci* **22**, 11272 (2021).
75. Yu, Y. *et al.* Purifying water with silver nanoparticles (AgNPs)-incorporated membranes: Recent advancements and critical challenges. *Water Res* **222**, 118901 (2022).
76. Sharif, M., Rahman, M. A., Ahmed, B., Abbas, R. Z. & Hassan, F. Copper Nanoparticles as Growth Promoter, Antioxidant and Anti-Bacterial Agents in Poultry Nutrition: Prospects and Future Implications. *Biol Trace Elem Res* **199**, 3825–3836 (2021).
77. Chatterjee, A. K., Chakraborty, R. & Basu, T. Mechanism of antibacterial activity of copper nanoparticles. *Nanotechnology* **25**, 135101 (2014).
78. Valdez-Salas, B. *et al.* Structure-activity relationship of diameter controlled Ag@Cu nanoparticles in broad-spectrum antibacterial mechanism. *Materials Science and Engineering: C* **119**, 111501 (2021).
79. Zahoor, M. *et al.* A Review on Silver Nanoparticles: Classification, Various Methods of Synthesis, and Their Potential Roles in Biomedical Applications and Water Treatment. *Water (Basel)* **13**, 2216 (2021).
80. Haider, Md. K., Kharaghani, D., Yoshiko, Y. & Kim, I. S. Lignin-facilitated growth of Ag/CuNPs on surface-activated polyacryloamidoxime nanofibers for superior antibacterial activity with improved biocompatibility. *Int J Biol Macromol* **242**, 124945 (2023).

81. Gonorrhoea (Neisseria gonorrhoeae infection). https://www.who.int/news-room/fact-sheets/detail/gonorrhoea-(neisseria-gonorrhoeae-infection) (2023).
82. Wall, K. M. *et al.* Etiologies of genital inflammation and ulceration in symptomatic Rwandan men and women responding to radio promotions of free screening and treatment services. *PLoS One* **16**, e0250044 (2021).
83. Disha, T. & Haque, F. Prevalence and Risk Factors of Vulvovaginal Candidosis during Pregnancy: A Review. *Infect Dis Obstet Gynecol* **2022**, 1–14 (2022).
84. Phillips, N. A., Rocktashel, M. & Merjanian, L. Ibrexafungerp for the Treatment of Vulvovaginal Candidiasis: Design, Development and Place in Therapy. *Drug Des Devel Ther* **Volume 17**, 363–367 (2023).
85. WHO releases new guidance to improve testing and diagnosis of sexually transmitted infections. https://www.who.int/news/item/24-07-2023-who-releases-new-guidance-to-improve-testing-and-diagnosis-of-sexually-transmitted-infections (2023).
86. Strickland, A. B. & Shi, M. Mechanisms of fungal dissemination. *Cellular and Molecular Life Sciences* **78**, 3219–3238 (2021).
87. Turner, S. A. & Butler, G. The Candida Pathogenic Species Complex. *Cold Spring Harb Perspect Med* **4**, a019778–a019778 (2014).
88. Talapko, J. *et al.* Candida albicans—The Virulence Factors and Clinical Manifestations of Infection. *Journal of Fungi* **7**, 79 (2021).
89. Silva, S., Rodrigues, C., Araújo, D., Rodrigues, M. & Henriques, M. Candida Species Biofilms' Antifungal Resistance. *Journal of Fungi* **3**, 8 (2017).
90. Bertini, M. Bacterial Vaginosis and Sexually Transmitted Diseases: Relationship and Management. in *Fundamentals of Sexually Transmitted Infections* (InTech, 2017). doi:10.5772/intechopen.69258.
91. Bashir, S. *et al.* Droplet-based microfluidic synthesis of silver nanoparticles stabilized by PVA and PVP: applications in anticancer and antimicrobial activities. *Chemical Papers* **76**, 7205–7216 (2022).
92. Lucío, M. I. *et al.* Bactericidal Effect of 5-Mercapto-2-nitrobenzoic Acid-Coated Silver Nanoclusters against Multidrug-Resistant *Neisseria gonorrhoeae*. *ACS Appl Mater Interfaces* **12**, 27994–28003 (2020).
93. Damelin, L. H., Fernandes, M. A. & Tiemessen, C. T. Alginate microbead-encapsulated silver complexes for selective delivery of broad-spectrum silver-based microbicides. *Int J Antimicrob Agents* **46**, 394–400 (2015).

94. Li, L.-H. *et al.* Non-Cytotoxic Nanomaterials Enhance Antimicrobial Activities of Cefmetazole against Multidrug-Resistant Neisseria gonorrhoeae. *PLoS One* **8**, e64794 (2013).
95. Jefferson, A., Smith, A., Fasinu, P. S. & Thompson, D. K. Sexually Transmitted Neisseria gonorrhoeae Infections—Update on Drug Treatment and Vaccine Development. *Medicines* **8**, 11 (2021).
96. Rojas-Jaimes, J. & Asmat-Campos, D. Cu2O, ZnO, and Ag/ Cu2O nanoparticles synthesized by biogenic and chemical route and their effect on Pseudomonas aeruginosa and Candida albicans. *Sci Rep* **13**, 21478 (2023).
97. Fan, X., Yahia, L. & Sacher, E. Antimicrobial Properties of the Ag, Cu Nanoparticle System. *Biology (Basel)* **10**, 137 (2021).
98. Eremenko, A. M., Petrik, I. S., Smirnova, N. P., Rudenko, A. V. & Marikvas, Y. S. Antibacterial and Antimycotic Activity of Cotton Fabrics, Impregnated with Silver and Binary Silver/Copper Nanoparticles. *Nanoscale Res Lett* **11**, 28 (2016).
99. Wierzbicki, M. *et al.* Evaluation of the Antimicrobial, Cytotoxic, and Physical Properties of Selected Nano-Complexes in Bovine Udder Inflammatory Pathogen Control. *Nanotechnol Sci Appl* **Volume 17**, 77–94 (2024).
100. Khalil, A. M., Hashem, A. H. & Kamel, S. Bimetallic hydrogels based on chitosan and carrageenan as promising materials for biological applications. *Biotechnol J* **18**, (2023).
101. Kamli, M. R. *et al.* Beta vulgaris Assisted Fabrication of Novel Ag-Cu Bimetallic Nanoparticles for Growth Inhibition and Virulence in Candida albicans. *Pharmaceutics* **13**, 1957 (2021).
102. Ye, Y. *et al.* Cell Wall Destruction and Internal Cascade Synergistic Antifungal Strategy for Fungal Keratitis. *ACS Nano* **16**, 18729–18745 (2022).
103. Pol, V. G. *et al.* Sonochemical Deposition of Silver Nanoparticles on Silica Spheres. *Langmuir* **18**, 3352–3357 (2002).
104. Chang, Z. *et al.* Janus silver mesoporous silica nanobullets with synergistic antibacterial functions. *Colloids Surf B Biointerfaces* **157**, 199–206 (2017).
105. Qasim, M., Singh, B. R., Naqvi, A. H., Paik, P. & Das, D. Silver nanoparticles embedded mesoporous SiO_2 nanosphere: an effective anticandidal agent against Candida albicans 077. *Nanotechnology* **26**, 285102 (2015).
106. Nuti, S. *et al.* Tailoring Mesoporous Silica-Coated Silver Nanoparticles and Polyurethane-Doped Films for Enhanced Antimicrobial Applications. *Nanomaterials* **14**, 462 (2024).
107. Araujo, V. H. S. *et al.* Nanosystems against candidiasis: a review of studies performed over the last two decades. *Crit Rev Microbiol* **46**, 508–547 (2020).

108. Cai, L. *et al.* Schiff-base silver nanocomplexes formation on natural biopolymer coated mesoporous silica contributed to the improved curative effect on infectious microbes. *Nano Res* **14**, 2735–2748 (2021).
109. Aati, S. *et al.* Silver-loaded mesoporous silica nanoparticles enhanced the mechanical and antimicrobial properties of 3D printed denture base resin. *J Mech Behav Biomed Mater* **134**, 105421 (2022).
110. Jo, J.-K. *et al.* Rechargeable microbial anti-adhesive polymethyl methacrylate incorporating silver sulfadiazine-loaded mesoporous silica nanocarriers. *Dental Materials* **33**, e361–e372 (2017).
111. Adamska, E., Niska, K., Wcisło, A. & Grobelna, B. Characterization and Cytotoxicity Comparison of Silver- and Silica-Based Nanostructures. *Materials* **14**, 4987 (2021).
112. Lee, J.-H. *et al.* Development of long-term antimicrobial poly(methyl methacrylate) by incorporating mesoporous silica nanocarriers. *Dental Materials* **32**, 1564–1574 (2016).
113. Kim, K.-J. *et al.* Antifungal activity and mode of action of silver nano-particles on Candida albicans. *BioMetals* **22**, 235–242 (2009).
114. Robles-Martínez, M. *et al.* Mentha piperita as a natural support for silver nanoparticles: A new Anti- Candida albicans treatment. *Colloid Interface Sci Commun* **35**, 100253 (2020).
115. Sun, L. *et al.* Synergy Between Polyvinylpyrrolidone-Coated Silver Nanoparticles and Azole Antifungal Against Drug-Resistant <I>Candida albicans</I> *J Nanosci Nanotechnol* **16**, 2325–2335 (2016).
116. Sy, K. *et al.* How Adding Chlorhexidine or Metallic Nanoparticles Affects the Antimicrobial Performance of Calcium Hydroxide Paste as an Intracanal Medication: An In Vitro Study. *Antibiotics* **10**, 1352 (2021).
117. Zhu, Y. *et al.* A facile route to prepare colorless Ag-Cu nanoparticle dispersions with elevated antibacterial effects. *Colloids Surf A Physicochem Eng Asp* **626**, 127116 (2021).
118. El-Batal, A. I. *et al.* Gum Arabic assisted the biomass synthesis of bimetallic silver copper oxide nanoparticles using gamma-rays for improving bacterial and viral wound healing: Promising antimicrobial activity against foot and mouth disease. *Int J Biol Macromol* **262**, 130010 (2024).
119. Długosz, O., Sochocka, M., Ochnik, M. & Banach, M. Metal and bimetallic nanoparticles: Flow synthesis, bioactivity and toxicity. *J Colloid Interface Sci* **586**, 807–818 (2021).
120. Chung, E. *et al.* Applied Methods to Assess the Antimicrobial Activity of Metallic-Based Nanoparticles. *Bioengineering* **10**, 1259 (2023).

121. Paszkiewicz, M. *et al.* Synthesis and Characterization of Monometallic (Ag, Cu) and Bimetallic Ag-Cu Particles for Antibacterial and Antifungal Applications. *J Nanomater* **2016**, 1–11 (2016).
122. Abou-El-Sherbini, K. S. *et al.* Encapsulation of Biosynthesized Nanosilver in Silica Composites for Sustainable Antimicrobial Functionality. *Global Challenges* **2**, (2018).
123. Zhang, N. C., Yu, X. & Ding, E. Y. Synthesis of Monodispersed Ag-Coated SiO₂ Nanoparticles with one-Pot Method and Investigation of its Antibacterial Activity. *Applied Mechanics and Materials* **117–119**, 940–943 (2011).
124. Rodrigues, M. C. *et al.* Biogenic synthesis and antimicrobial activity of silica-coated silver nanoparticles for esthetic dental applications. *J Dent* **96**, 103327 (2020).
125. Priebe, M. *et al.* Antimicrobial silver-filled silica nanorattles with low immunotoxicity in dendritic cells. *Nanomedicine* **13**, 11–22 (2017).
126. Dhanalekshmi, K. I. & Meena, K. S. Comparison of antibacterial activities of Ag@TiO2 and Ag@SiO2 core–shell nanoparticles. *Spectrochim Acta A Mol Biomol Spectrosc* **128**, 887–890 (2014).
127. Otari, S. V. *et al.* Facile one pot synthesis of core shell Ag@SiO2 nanoparticles for catalytic and antimicrobial activity. *Mater Lett* **167**, 179–182 (2016).
128. Isaacs, M. A. *et al.* Tunable Ag@SiO_2 core–shell nanocomposites for broad spectrum antibacterial applications. *RSC Adv* **7**, 23342–23347 (2017).
129. Ertem, E. *et al.* Core–Shell Silver Nanoparticles in Endodontic Disinfection Solutions Enable Long-Term Antimicrobial Effect on Oral Biofilms. *ACS Appl Mater Interfaces* **9**, 34762–34772 (2017).
130. Acharya, D., Mohanta, B., Pandey, P. & Nasiri, F. Antibacterial properties of synthesized Ag and Ag@SiO_2 core–shell nanoparticles: a comparative study. *Can J Phys* **96**, 955–960 (2018).
131. Selvan, D. S. A., Shobana, S., Thiruvasagam, P., Murugesan, S. & Rahiman, A. K. Evaluation of Antimicrobial and Antidiabetic Activities of Ag@SiO2 Core–Shell Nanoparticles Synthesized with Diverse Shell Thicknesses. *J Clust Sci* **31**, 739–749 (2020).
132. Lino, M. M., Paulo, C. S. O., Vale, A. C., Vaz, M. F. & Ferreira, L. S. Antifungal activity of dental resins containing amphotericin B-conjugated nanoparticles. *Dental Materials* **29**, e252–e262 (2013).
133. Paulo, C. S. O., Lino, M. M., Matos, A. A. & Ferreira, L. S. Differential internalization of amphotericin B – Conjugated nanoparticles in human cells and the expression of heat shock protein 70. *Biomaterials* **34**, 5281–5293 (2013).

134. Paulo, C. S. O., Vidal, M. & Ferreira, L. S. Antifungal Nanoparticles and Surfaces. *Biomacromolecules* **11**, 2810–2817 (2010).
135. Zhang, J., Li, X., Rosenholm, J. M. & Gu, H. Synthesis and characterization of pore size-tunable magnetic mesoporous silica nanoparticles. *J Colloid Interface Sci* **361**, 16–24 (2011).
136. Frank, A. J., Cathcart, N., Maly, K. E. & Kitaev, V. Synthesis of Silver Nanoprisms with Variable Size and Investigation of Their Optical Properties: A First-Year Undergraduate Experiment Exploring Plasmonic Nanoparticles. *J Chem Educ* **87**, 1098–1101 (2010).
137. Wiley, B., Sun, Y. & Xia, Y. Synthesis of Silver Nanostructures with Controlled Shapes and Properties. *Acc Chem Res* **40**, 1067–1076 (2007).
138. Millstone, J. E., Hurst, S. J., Métraux, G. S., Cutler, J. I. & Mirkin, C. A. Colloidal Gold and Silver Triangular Nanoprisms. *Small* **5**, 646–664 (2009).
139. Djafari, J. *et al.* Exploring the control in antibacterial activity of silver triangular nanoplates by surface coating modulation. *Front Chem* **7**, (2019).
140. Fernández-Lodeiro, C. *et al.* Adenosine-Monophosphate-Assisted Homogeneous Silica Coating of Silver Nanoparticles in High Yield. *Nanomaterials* **13**, 2788 (2023).
141. Carvalho, G. C. *et al.* Cetyltrimethylammonium bromide in the synthesis of mesoporous silica nanoparticles: General aspects and in vitro toxicity. *Advances in Colloid and Interface Science* vol. 307 Preprint at https://doi.org/10.1016/j.cis.2022.102746 (2022).
142. Lang, N. & Tuel, A. A fast and efficient ion-exchange procedure to remove surfactant molecules from MCM-41 materials. *Chemistry of Materials* **16**, 1961–1966 (2004).
143. Zhang, M. *et al.* Fabrication of mesoporous silica-coated CNTs and application in size-selective protein separation. *J Mater Chem* **20**, 5835 (2010).
144. Oliveira, E. *et al.* Sustainable synthesis of luminescent CdTe quantum dots coated with modified silica mesoporous nanoparticles: Towards new protein scavengers and smart drug delivery carriers. *Dyes and Pigments* **161**, 360–369 (2019).
145. Ahangaran, F., Hassanzadeh, A. & Nouri, S. Surface modification of Fe3O4@SiO2 microsphere by silane coupling agent. *Int Nano Lett* **3**, 23 (2013).
146. Kaasalainen, M. *et al.* Size, Stability, and Porosity of Mesoporous Nanoparticles Characterized with Light Scattering. *Nanoscale Res Lett* **12**, (2017).
147. Ndayishimiye, J. *et al.* Engineering mesoporous silica nanoparticles towards oral delivery of vancomycin. *J Mater Chem B* **9**, 7145–7166 (2021).
148. Thommes, M. Physical Adsorption Characterization of Nanoporous Materials. *Chemie Ingenieur Technik* **82**, 1059–1073 (2010).

149. Thommes, M. *et al.* Physisorption of gases, with special reference to the evaluation of surface area and pore size distribution (IUPAC Technical Report). *Pure and Applied Chemistry* **87**, 1051–1069 (2015).
150. Thommes, M. & Cychosz, K. A. Physical adsorption characterization of nanoporous materials: progress and challenges. *Adsorption* **20**, 233–250 (2014).
151. Huang, X., Young, N. P. & Townley, H. E. Characterization and Comparison of Mesoporous Silica Particles for Optimized Drug Delivery. *Nanomaterials and Nanotechnology* **4**, 2 (2014).
152. Soto, R., Patel, P., Albadarin, A. B., Diniz, M. O. & Hudson, S. P. Solubility, aggregation and stability of Amphotericin B drug in pure organic solvents: Thermodynamic analysis and solid form characterization. *J Mol Liq* **366**, 120276 (2022).
153. Grela, E. *et al.* Modes of the antibiotic activity of amphotericin B against Candida albicans. *Sci Rep* **9**, 17029 (2019).
154. Montenegro, M. *et al.* Methodology Development and Validation of Amphotericin B Stability by HPLC-DAD. *J Braz Chem Soc* (2020) doi:10.21577/0103-5053.20190256.
155. Alencar, É. N., Sawangchan, P., Kirsch, L. E. & Egito, E. S. T. Unveiling the Amphotericin B Degradation Pathway and Its Kinetics in Lipid-Based Solutions. *J Pharm Sci* **110**, 1248–1258 (2021).
156. Lim, C. *et al.* Preparation, Characterization, and In Vivo Pharmacokinetic Study of the Supercritical Fluid-Processed Liposomal Amphotericin B. *Pharmaceutics* **11**, 589 (2019).
157. Mouton, J. W., Meletiadis, J., Voss, A. & Turnidge, J. Variation of MIC measurements: the contribution of strain and laboratory variability to measurement precision. *Journal of Antimicrobial Chemotherapy* **73**, 2374–2379 (2018).
158. Kowalska-Krochmal, B. & Dudek-Wicher, R. The Minimum Inhibitory Concentration of Antibiotics: Methods, Interpretation, Clinical Relevance. *Pathogens* **10**, 165 (2021).
159. Sterling, T. R. & Merz, W. G. Resistance to amphotericin B: emerging clinical and microbiological patterns. *Drug Resistance Updates* **1**, 161–165 (1998).
160. Cordeiro, R. A. *et al.* Minimum inhibitory concentrations of amphotericin B, azoles and caspofungin against *Candida* species are reduced by farnesol. *Med Mycol* **51**, 53–59 (2013).
161. Teixeira, M. V. S., Aldana-Mejía, J. A., da Silva Ferreira, M. E. & Furtado, N. A. J. C. Lower Concentrations of Amphotericin B Combined with Ent-Hardwickiic Acid Are Effective against Candida Strains. *Antibiotics* **12**, 509 (2023).

162. Adediran, S. A. *et al.* Synthesis of a Highly Water-Soluble Derivative of Amphotericin B with Attenuated Proinflammatory Activity. *Mol Pharm* **6**, 1582–1590 (2009).
163. Abu Ammar, A. *et al.* Amphotericin B-loaded nanoparticles for local treatment of cutaneous leishmaniasis. *Drug Deliv Transl Res* **9**, 76–84 (2019).
164. Yan, Y., Liao, Z., Shen, J., Zhu, Z. & Cao, Y. Nicotinamide potentiates amphotericin B activity against *Candida albicans*. *Virulence* **13**, 1533–1542 (2022).
165. Khan, S. N. *et al.* Synergistic fungicidal activity with low doses of eugenol and amphotericin B against Candida albicans. *Biochem Biophys Res Commun* **518**, 459–464 (2019).
166. Pfaller, M. A. *et al.* Wild-Type MIC Distributions and Epidemiological Cutoff Values for Amphotericin B, Flucytosine, and Itraconazole and Candida spp. as Determined by CLSI Broth Microdilution. *J Clin Microbiol* **50**, 2040–2046 (2012).
167. Lee, H. *et al.* Comparison of Six Antifungal Susceptibilities of 11 *Candida* Species Using the VITEK2 AST–YS08 Card and Broth Microdilution Method. *Microbiol Spectr* **10**, (2022).
168. Gür Vural, D., Çetin, G., Bilgin, K., Tanrıverdi Çaycı, Y. & Birinci, A. Determination of amphotericin B antifungal susceptibility in Candida strains using an inverted microscope. *The Journal of Infection in Developing Countries* **18**, 303–308 (2024).
169. Uroro, E. O., Bright, R., Hayles, A. & Vasilev, K. Lipase-Responsive Amphotericin B Loaded PCL Nanoparticles for Antifungal Therapies. *Nanomaterials* **13**, 155 (2022).
170. Esposito, E. Amphiphilic association systems for Amphotericin B delivery. *Int J Pharm* **260**, 249–260 (2003).
171. Alves, R. *et al.* Adapting to survive: How Candida overcomes host-imposed constraints during human colonization. *PLoS Pathogens* vol. 16 Preprint at https://doi.org/10.1371/journal.ppat.1008478 (2020).
172. Du, H. & Huang, G. Environmental pH adaption and morphological transitions in Candida albicans. *Current Genetics* vol. 62 283–286 Preprint at https://doi.org/10.1007/s00294-015-0540-8 (2016).
173. Hinton, M. *MUELLER-HINTON BROTH CULTURE OF MICROORGANISMS 1 INTENDED USE*. vol. 3 www.biokar-diagnostics.com.
174. Cayman Chemical. Amphotericin B - Product info. (2022).
175. Dou, Q., Li, Y., Wong, K. W. & Ng, K. M. Facile synthesis of nearly monodisperse AgCu alloy nanoparticles with synergistic effect against oxidation and electromigration. *J Mater Res* **34**, 2095–2104 (2019).

176. Tao, Y., Zhou, F., Wang, K., Yang, D. & Sacher, E. AgCu NP Formation by the Ag NP Catalysis of Cu Ions at Room Temperature and Their Antibacterial Efficacy: A Kinetic Study. *Molecules* **27**, 6951 (2022).
177. Kim, N. R., Shin, K., Jung, I., Shim, M. & Lee, H. M. Ag–Cu Bimetallic Nanoparticles with Enhanced Resistance to Oxidation: A Combined Experimental and Theoretical Study. *The Journal of Physical Chemistry C* **118**, 26324–26331 (2014).
178. MEDSAFE. AmBisomeinj. *https://www.medsafe.govt.nz/profs/datasheet/a/AmBisomeinj.pdf* (2017).
179. DailyMed. Amphotericin B - XGen Pharms. *https://dailymed.nlm.nih.gov/dailymed/drugInfo.cfm?setid=a0a54943-9ce4-4f3e-b681-a1a9144c16ce* (2022).
180. DailyMed. AmphotericinB - Eugia US LLC. *https://dailymed.nlm.nih.gov/dailymed/drugInfo.cfm?setid=6f24975c-5191-4fc2-a8da-e57358f8e154* (2022).